Neuron
Article

The Cell-Intrinsic Requirement of *Sox6* for Cortical Interneuron Development

Renata Batista-Brito,[1,2] Elsa Rossignol,[1,6] Jens Hjerling-Leffler,[1,6] Myrto Denaxa,[3] Michael Wegner,[4] Véronique Lefebvre,[5] Vassilis Pachnis,[3] and Gord Fishell[1,*]

[1]Smilow Neuroscience Program and the Department of Cell Biology, Smilow Research Building, New York University School of Medicine, 522 First Avenue, New York, NY 10016, USA

[2]Gulbenkian Ph.D. Program in Biomedicine, Gulbenkian Science Institute, 2781-901 Oeiras, Portugal

[3]Division of Molecular Neurobiology, MRC, National Institute for Medicine Research, Mill Hill, London, NW7 1AA, UK

[4]Institut fuer Biochemie, Universitaet Erlangen-Nuernberg, Fahrstrasse 17, 91054 Erlangen, Germany

[5]Department of Cell Biology and Orthopaedic Research Center, Cleveland Clinic Lerner Research Institute, 9500 Euclid Avenue (NC10), Cleveland, OH 44195, USA

[6]These authors contributed equally to this work

*Correspondence: fisheg01@nyumc.org

DOI 10.1016/j.neuron.2009.08.005

SUMMARY

We describe the role of Sox6 in cortical interneuron development, from a cellular to a behavioral level. We identify Sox6 as a protein expressed continuously within MGE-derived cortical interneurons from postmitotic progenitor stages into adulthood. Both its expression pattern and null phenotype suggests that *Sox6* gene function is closely linked to that of *Lhx6.* In both *Lhx6* and *Sox6* null animals, the expression of PV and SST and the position of both basket and Martinotti neurons are abnormal. We find that Sox6 functions downstream of *Lhx6.* Electrophysiological analysis of *Sox6* mutant cortical interneurons revealed that basket cells, even when mispositioned, retain characteristic but immature fast-spiking physiological features. Our data suggest that Sox6 is not required for the specification of MGE-derived cortical interneurons. It is, however, necessary for their normal positioning and maturation. As a consequence, the specific removal of *Sox6* from this population results in a severe epileptic encephalopathy.

INTRODUCTION

Since the pioneering work of Ramon y Cajal in the last century, cortical interneuron populations have been recognized to be particularly diverse in terms of their morphology, intrinsic properties, and connectivity. This heterogeneity of interneuron subtypes is thought to enable them to contribute differentially to various higher brain functions (Glickfeld et al., 2009; Szabadics et al., 2006; Tamas et al., 2003). During development, cortical interneurons have been implicated in the assembly of cortical networks and the emergent properties of the brain. For instance, one of the earliest coherent forms of brain activity, giant depolarizing potentials, is dependent on the activity of GABAergic interneurons (Allene et al., 2008). Efforts to determine the contribution of specific interneuron subtypes to network development have been hampered by the fact that cortical interneuron classification is based on mature properties not yet present during these early events. However, recent findings show that the expression of genetic programs specific for the place and time of origin of the cells correlate with their mature properties (for review see Batista-Brito et al., 2009).

All cortical interneurons, at least in nonprimate mammals, are derived from the subpallium of the telencephalon (Corbin et al., 2001; Kriegstein and Noctor, 2004; Marin and Rubenstein, 2001, 2003). In particular, they mainly arise from two telencephalic transient embryonic structures, the medial and caudal ganglionic eminences (the MGE and CGE, respectively) (Anderson et al., 2001; Nery et al., 2002; Sussel et al., 1999). Fate-mapping studies have shown that the cortical interneuron subtypes arising from these two sources are mutually exclusive (Butt et al., 2005; Fogarty et al., 2007; Nery et al., 2002; Xu et al., 2008). While the MGE gives rise to the fast-spiking (FS) basket cells and Martinotti interneurons, the CGE is the source of the bipolar and neurogliaform populations (Butt et al., 2005; G.F., unpublished data). This suggests that distinct genetic programs are initiated within the MGE and CGE interneuron progenitors. Indeed, numerous genes expressed throughout the ventricular and subventricular zones (VZ and SVZ, respectively) appear to contribute to the specification, migration, and differentiation of cortical interneuron populations. These include genes with widespread expression throughout the subpallium, such as *Mash1,* the *Dlx* family of genes (*Dlx1*, *2*, *5*, and *6*) (Anderson et al., 1997a, 1997b; Cobos et al., 2005; Ghanem et al., 2007; Potter et al., 2009), *Met* (Powell et al., 2001), *Olig2* (Miyoshi et al., 2007b), and *Gsh2* (Corbin et al., 2000; Fogarty et al., 2007; Stenman et al., 2003), as well as a series of transcription-factor-encoding genes with more restricted subpallial regional expression, such as *Nkx2-1* (Butt et al., 2008; Du et al., 2008; Nobrega-Pereira et al., 2008; Sussel et al., 1999; Xu et al., 2008), *Lhx6* (Alifragis et al., 2004; Cobos et al., 2006; Du et al., 2008; Fogarty et al., 2007; Liodis et al., 2007; Zhao et al., 2008), *Lhx7* (Fragkouli et al., 2005; Zhao et al., 2003), *Nkx6.2* (Fogarty et al., 2007; Sousa et al., 2009), and *CoupTFII* (Kanatani et al., 2008; Tripodi et al., 2004). These latter genes are attractive candidates

for regulating the specification of particular cortical interneuron subclasses.

In particular, *Nkx2-1* has been shown to repress the program utilized by CGE-derived cortical interneuron populations while simultaneously promoting the development of MGE-derived cortical interneurons (Butt et al., 2008; Sussel et al., 1999). Recent work suggests that *Lhx6* is an essential downstream effector of Nkx2-1 activity (Du et al., 2008). In accordance, loss-of-function analysis of an *Lhx6* null allele indicates that this gene is required for the positioning and maturation of MGE-derived cortical interneuron populations (Liodis et al., 2007; Zhao et al., 2008). However, other effector genes that act downstream of *Nkx2-1* and *Lhx6* have yet to be identified.

In an attempt to better address the molecular mechanisms utilized in the generation of cortical interneuron subclasses, a number of laboratories, including our own, have undertaken genome-wide microarray analyses of the genes expressed within developing cortical interneurons (Batista-Brito et al., 2009; Marsh et al., 2008; Okaty et al., 2009). Through this approach the Sry-related HMG-box-containing transcription factor *Sox6* was identified. This gene has been previously implicated as being involved in cell fate commitment in cartilage and oligodendrogenesis, thus suggesting that it might regulate cell fate in interneurons as well. Indeed, a very recently published paper found as we did that *Sox6* is expressed and required in MGE-derived cortical interneurons, and in addition plays an independent role in pallial/subpallial patterning (Azim et al., 2009). Recent work by the same group has also identified *Sox5*, a close homolog of *Sox6*, as being required for the specification of deep layer pyramidal neurons in layer V and VI of the cortex (Lai et al., 2008). Here we demonstrate that Sox6 is present in most if not all MGE-derived neurons in the mature brain and appears to function genetically downstream of *Lhx6*. Moreover we show that Sox6 is required for the positioning and maturation of FS basket cells, and to a lesser extent, Martinotti cells. We demonstrate that these cellular abnormalities result in the development of a progressive and severe epileptic encephalopathy.

RESULTS

Migrating Cortical Interneurons Express *Sox6*

We identified Sox6 in a previous microarray analysis as being expressed in cortical interneurons (Batista-Brito et al., 2009). In order to analyze the expression of Sox6, we used the paninterneuron transgenic line *Dlx5/6^{Cre};RCE$^{EGFP/+}$*, which allows the permanent labeling of interneurons with EGFP through Cre-mediated recombination of the RCE reporter. Immunocytochemistry of Sox6 demonstrated that migrating cortical interneurons express this protein at all of the analyzed time points (E12.5, E13.5: data not shown; E14.5: Figures 1A and 1A′). Furthermore, *Sox6* is also expressed in other cortical populations, particularly within the VZ of the dorsal telencephalon (Figure 1A).

Due to the high degree of similarity between *Sox6* and *Sox5* (Lefebvre et al., 2007; Lai et al., 2008), we tested if Sox5 was expressed in migrating cortical interneurons (Figures 1B and 1B′). While Sox5 is expressed in postmitotic pyramidal cells, it is excluded from cortical interneurons. Indeed, our analysis revealed that Sox5 and Sox6 expression is complementary within the neocortex (c.f. Figures 1A′and 1B′).

To determine whether Sox6 is expressed within a specific subpopulation of cortical interneurons, we used genetic fate-mapping and immunocytochemical colocalization to examine its overlap with Lhx6, a marker of MGE-derived cortical interneuronal lineages (Cobos et al., 2006; Du et al., 2008; Fogarty et al., 2007; Liodis et al., 2007), (Figures 1C and 1D). Sox6 and Lhx6 are extensively colocalized within the MGE, with the vast majority of Lhx6-expressing cells also being Sox6 positive (Figure 1C: 94% ± 6% based on the colocalization of EGFP and Sox6 in *Lhx6^{cre};RCE$^{EGFP/+}$* mice). However, while Sox6 is highly expressed in postmitotic migrating interneurons, its level of expression is lower within the MGE (Figure 1D′), in contrast to Lhx6 whose levels are similar in both proliferative and migrating interneurons (Figures 1D′ and 1D″).

To determine if Sox6-expressing cells are mitotic, we examined the expression of the proliferation marker Ki-67 (Kill, 1996; Figure 1E). In the ventral telencephalon only a small percentage of Sox6 cells were undergoing proliferation within the SVZ (Figure 1E′). In contrast, Sox6-expressing cells within the cortical VZ uniformly express Ki-67, suggesting that Sox6 is expressed in all the progenitors giving rise to pyramidal cell lineages (Figure 1E″).

Sox6 Is Expressed in Mature MGE-Derived Cortical Interneurons

By fate-mapping cortical interneurons using a paninterneuron transgenic labeling strategy, *Dlx5/6^{Cre};RCE$^{EGFP/+}$*, we determined that 62% ± 3% (n = 3) of interneurons within the P21 cortex express Sox6 (Figures 2A and 2F). We also detected extensive Sox6 labeling in hippocampal interneurons (Figure 2B). While the vast majority of Sox6 cells in the cortex are interneurons, most of the remaining ones express Olig2 (data not shown).

In the murine somatosensory cortex, parvalbumin (PV), somatostatin (SST), and vasoactive intestinal polypeptide (VIP) are expressed in mutually exclusive populations of cortical interneurons (Kawaguchi, 1995; Kubota et al., 1994; Miyoshi et al., 2007a). By genetic fate-mapping it has recently been demonstrated that PV- and SST-expressing interneurons are exclusively derived from the MGE, while VIP cells do not come from that lineage (Fogarty et al., 2007; Xu et al., 2004). By contrast, calretinin (CR)- and NPY- labeled interneuron populations derive from both the MGE and the CGE (Butt et al., 2005; Fogarty et al., 2007; Xu et al., 2004). Hence, we performed coimmunohistochemistry for Sox6 and these interneuron markers (Figures 2C–2F, n = 3). This analysis revealed that the vast majority of PV- (93% ± 4%) and SST-expressing (94% ± 6%) interneurons are Sox6 positive, while virtually all the VIP interneurons are Sox6 negative (2% ± 1%). Furthermore, we found that 40% ± 4% of NPY interneurons, and 19% ± 2% of CR interneurons, coexpress Sox6. Taken together, these results demonstrate that Sox6 is expressed in most mature MGE-derived interneurons.

Sox6 Loss of Function

Sox6 null mice are generally born alive, but the majority of them die within 1 hr of birth from unknown causes (Smits et al., 2001). A very small percentage of *Sox6* null mice live up to P10–P11;

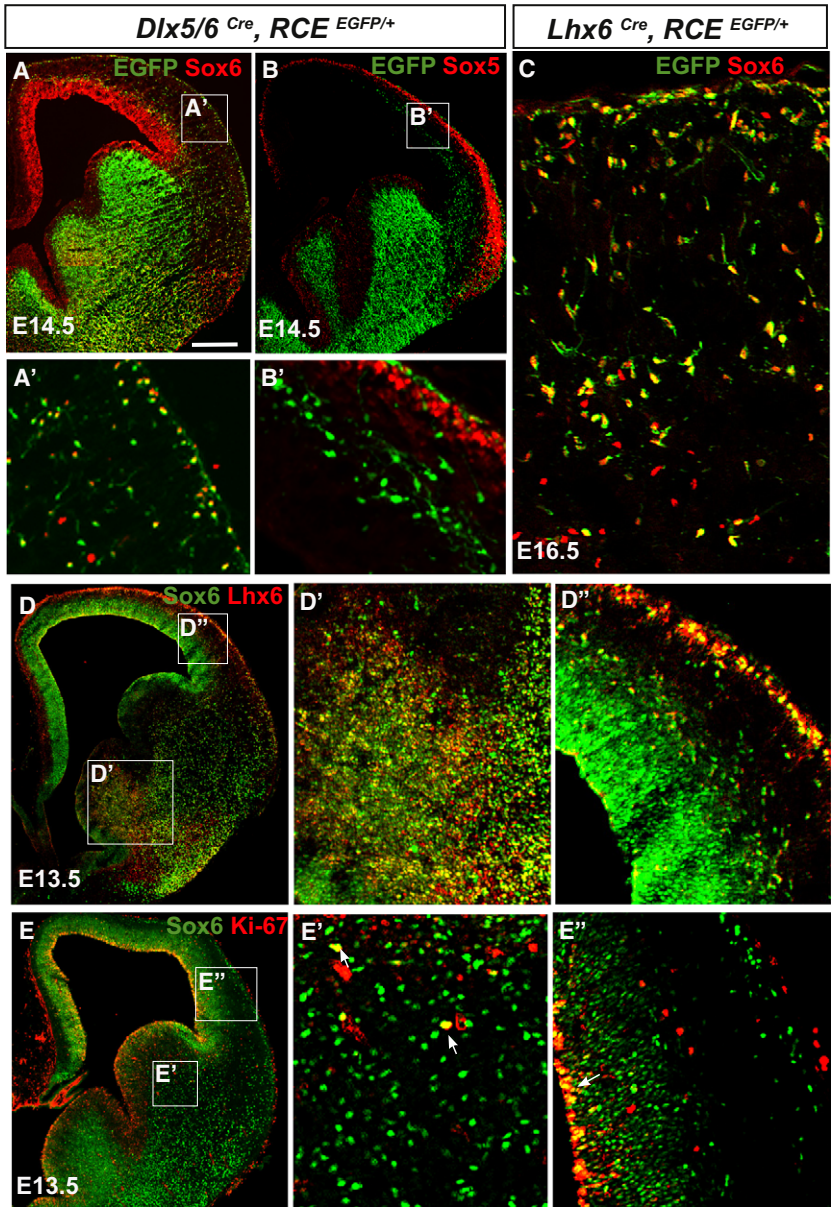

Figure 1. Sox6 Is Primarily Expressed In Post-mitotic Lhx6-Expressing Cortical Interneurons

(A) To assess if migrating cortical interneurons express Sox6, coronal telencephalic sections from *Dlx5/6*^{Cre};*RCE*$^{EGFP/+}$ mice were analyzed at E14.5. (A) Sox6 (red)/EGFP (green) double/labeled cells were observed in the mantle of the ventral telencephalon. Many of the interneurons in the cortex with morphologies suggesting active migration express Sox6; however, some Sox6-expressing cells do not express EGFP (for details see A′). The dorsal VZ also expresses Sox6.

(B) In contrast, migrating cortical interneurons do not express Sox5 (red).

(C) To assess if Sox6 (red) is expressed within the MGE-derived lineage, we fate-mapped MGE interneurons using the *Lhx6*^{Cre};*RCE*$^{EGFP/+}$ (green) line. Virtually all *Lhx6*-lineage cortical interneurons express Sox6 (94% ± 6%).

(D) The extent of colocalization of Sox6 (green) and Lhx6 (red) was also analyzed by antibody staining at E13.5. Consistent with our genetic fate-mapping of this population, most (if not all) Lhx6 cells are also Sox6 positive; however, the relative levels of expression of these two proteins vary. Sox6, while expressed at low levels in the MGE (D′), becomes highly expressed in migrating interneurons within the mantle and the cortex (D″).

(E) To test if Sox6 cells are actively proliferating, we examined whether there exists coexpression of Sox6 (green) and the proliferation marker Ki-67 (red). Within the ventral telencephalon, while a few cells were double positive (arrowheads in E′), indicating proliferation, most of the Sox6 cells did not express Ki-67. In the cortex (E′), Sox6 colocalizes with Ki-67 exclusively in the ventricular zone (arrow in E″). (A′)–(E″) correspond to the area outlined by the white squares in (A)–(E), respectively.

n = 3 for each experimental condition. Scale bar in (A) corresponds to 400 μm in (A) and (B), 40 μm in (C), and 500 μm in (D) and (E).

however, these mice are consistently smaller and weaker than their control littermates. To test the functional role of *Sox6* in cortical interneurons, we began by analyzing the surviving *Sox6* null mice (*Sox6*$^{-/-}$) at P10–P11. Preliminary data suggest that the total number of cortical interneurons, as assessed by *Gad67* expression, is not obviously affected (Figures S1A and S1B available online), while the amount of interneuron markers PV and SST appears to be decreased and the number of NPY-expressing cells appears to be increased (results not shown). In contrast, VIP expression does not appear to be affected. These findings are consistent with a similar analysis examining the role of *Sox6* in these same contexts (Azim et al., 2009).

The most striking of these findings was the loss of PV expressing cells. However, given the late initiation of expression of this protein (approximately P12 in wild-type cortical basket cells) coupled with the high level of lethality in the mutant, it is difficult to know whether these observations reflect a loss of this population or simply their failure to mature in *Sox6* mutant mice. Hence we sought to examine the effect of conditional ablation of *Sox6* specifically within the MGE-derived cortical interneuron populations. By using the *Lhx6*^{Cre} driver in combination with a *Sox6*$^{F/F}$ conditionally null allele, we were able to restrict the removal of *Sox6* solely to the MGE-derived population (Fogarty et al., 2007). The intersection of *Lhx6* and *Sox6* expression allows exquisite specificity for testing the function of *Sox6* within cortical interneurons derived from the MGE. By including the *RCE*$^{EGFP/+}$ reporter line (Sousa et al., 2009) in our analysis, we were able to fate-map the *Lhx6*/*Sox6*-expressing cells in both controls (*Sox6*$^{F/+}$;*Lhx6*^{Cre};*RCE*$^{EGFP/+}$) and conditional mutants (*Sox6*$^{F/F}$;*Lhx6*^{Cre};*RCE*$^{EGFP/+}$). Moreover, by examining the EGFP-negative cortical interneuron population, we could gauge the non-cell-autonomous consequences of loss of *Sox6* on CGE lineages. *Sox6*$^{F/F}$;

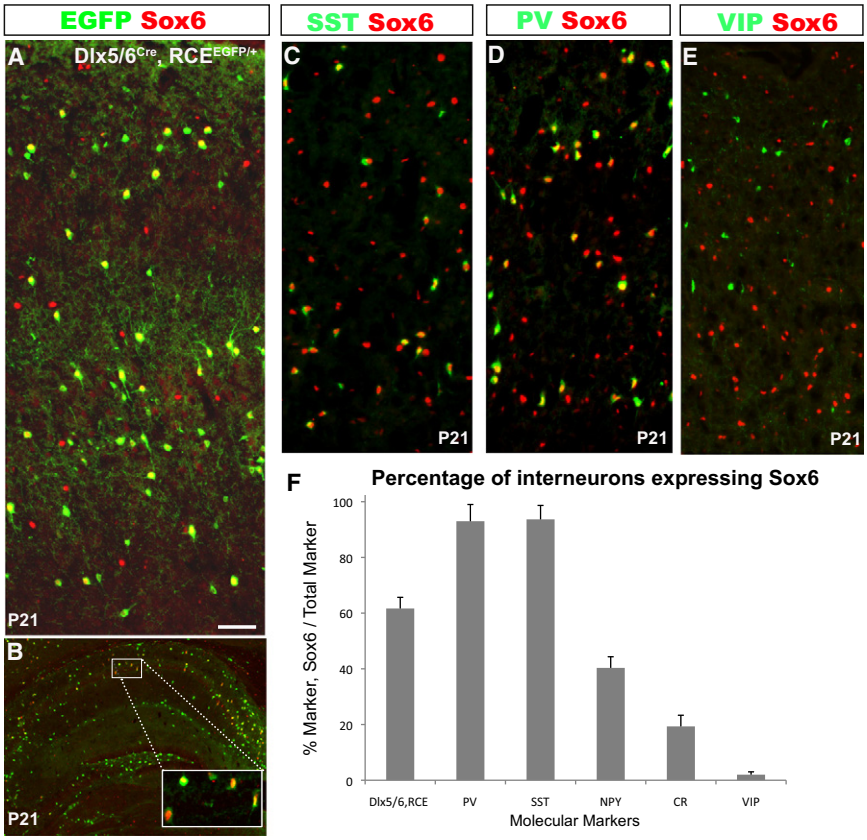

Figure 2. Sox6 Is Expressed in Mature MGE-Derived Cortical Interneurons

(A and B) In order to determine the percentage of cortical interneurons that express Sox6 at P21, telencephalic coronal sections from *Dlx5/6*^{Cre}*;RCE*$^{EGFP/+}$ mice were analyzed. (A) Within the somatosensory cortex, 62% ± 3% of the total number of interneurons (EGFP; green) express Sox6 (red). (B) A subset of hippocampal interneurons also express Sox6 (box in B shows a higher-power view of the region indicated).

(C–F) To determine the percentage of each interneuron subtype that expresses Sox6, coronal sections of somatosensory cortex were analyzed at P21. (C–E) Representative examples of double immunostaining for Sox6 (red), and SST, PV, or VIP (green). (C and D) The majority of PV and SST cells coexpress Sox6. (E) We observed virtually no colocalization between Sox6 (red) and VIP (green). (F) The percentage of fate-mapped *Dlx5/6*^{Cre}*;RCE*$^{EGFP/+}$ interneurons that express Sox6 (62% ± 3%), and the percentages of specific cortical interneuron subtypes that coexpress Sox6 and the following markers: PV (93% ± 4%); SST (94% ± 6%); NPY (40% ± 4%); and CR (19% ± 2%). In contrast, very few VIP interneurons express Sox6 (2% ± 1%).

n = 3. Scale bar in (A) corresponds to 40 μm in (A), 60 μm in (B), and 50 μm in (C–E).

Lhx6^{Cre}*;RCE*$^{EGFP/+}$ animals generally resembled their nonmutant littermates up to approximately P15. However, they subsequently failed to thrive and developed a severe seizure disorder, ultimately resulting in death between the ages of P17–P19.

Sox6 Is Necessary for Cortical Interneuron Migration and Laminar Positioning

Sox6$^{F/F}$*;Lhx6*^{Cre}*;RCE*$^{EGFP/+}$ mutant cells did not show any obvious defect in tangential migration (c.f Figures 3A–3D with Lavdas et al., 1999; Marin and Rubenstein, 2001). Upon reaching the cortex, interneurons shift to a radial mode of migration as they enter the cortical plate (Ang et al., 2003; Polleux et al., 2002). Our data appear to indicate that conditionally null *Sox6* interneurons have a defect in their ability to transition from tangential to radial migration. Consequently they accumulate in the marginal and intermediate zones (MZ and IZ, respectively). To provide landmarks for specific cortical laminae, we used the perinatally expressed transcription factors Ctip2 (Figures 3A, 3B, 3E, and 3F), which is expressed in layer V and at lower levels in layer VIa (Arlotta et al., 2005; Chen et al., 2008), and Tbr1 (Figures 3C, 3D, 3G, and 3H), which is expressed in layer VIa (Hevner et al., 2001). Postnatally, mutant *Sox6* interneurons (*Sox6*$^{F/F}$*;Lhx6*^{Cre}*;RCE*$^{EGFP/+}$) accumulate in layers I and VI, apparently at the expense of layers II, III, and IV (Figures 3I, 3J, and 4A–4D: layer I: control [0.5% ± 0.3%] versus mutant [17% ± 6%]; layer II/III: control [20% ± 3%] versus mutant [15% ± 3%]; layer IV: control [16% ± 3%] versus mutant [5% ± 3%]; layer V: control [31% ± 4%] versus mutant [22% ± 5%]; and layer VI: control [28% ± 4%] versus mutant [36% ± 8%]). This population is normally absent from layer I as shown in control littermates (Figures 3E, 3G, 3I, and 4). Indeed, normally the only cortical interneurons in this layer are CGE-derived (G.F., unpublished data), and there is a small population of NPY interneurons derived from the preoptic area (Gelman et al., 2009). Hence, at P17–P19, although redistributed (Figure 4), the total number of fate-mapped interneurons is only 18% ± 12% decreased (Figure 3J). The mutant cells do however appear to retain their GABAergic interneuron character, as their expression of *Gad67* persists. However, we observed a 19% ± 11% reduction in this population, which is comparable to the observed decrease in the number of fate-mapped neurons (Figures 4G and 4H).

Sox6 Mutant Interneurons Retain Their Identity but Fail to Mature

We next performed double immunostainings for EGFP and multiple molecular markers characteristically expressed by different cortical interneuron subtypes (Figures 4 and 5, n = 5). The most dramatic effects observed in the mutant population were a marked decrease in PV expression (by 94% ± 3%; Figures 4A, 4B, 5A, and 5G) and a concomitant increase in NPY expression (by 77% ± 6%; Figures 4C–4F, 4I, 4J, 5C, and 5G). There was also a 30% ± 2% reduction in the SST-expressing fate-mapped population and more specifically a complete loss of the SST/CR double-positive subtype (Figures 5B, 5D, and 5G). The percentage of fate-mapped interneurons expressing the molecular markers Kv3.1b (normally expressed in PV-FS

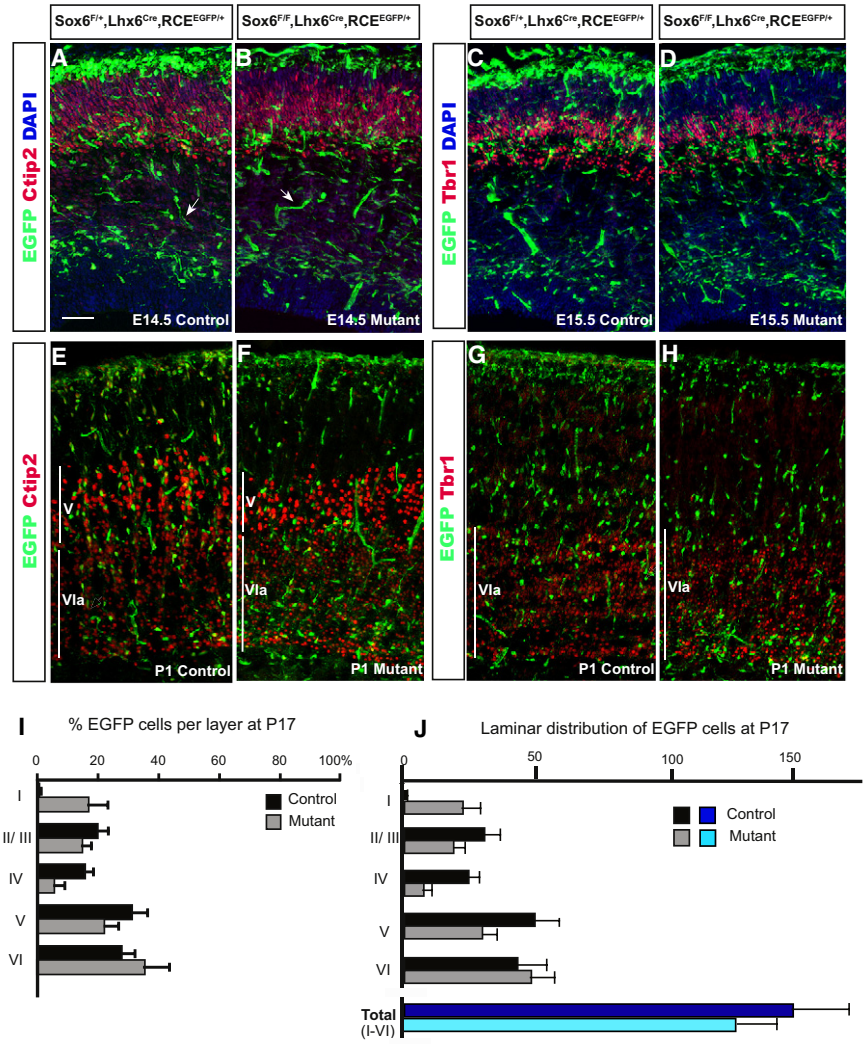

Figure 3. Sox6 Mutant MGE-Derived Interneurons Have Migratory Defects Resulting in General Restriction to the Most Superficial and Deep Cortical Layers

(A and D) In order to determine if *Sox6* affects interneuron migration, we fate-mapped (A, C, E, and G) *Sox6* control ($Sox6^{F/+};Lhx6^{Cre};RCE^{EGFP/+}$) (green) and (B, D, F, and H) mutant interneurons ($Sox6^{F/F};Lhx6^{Cre};RCE^{EGFP/+}$) during embryonic development (A–D) and at P1 (E–H). The specific cortical laminae were visualized using Ctip2 (red) (which is expressed at high levels in layer V and weakly in layer VIa at perinatal ages; Arlotta et al., 2005; Chen et al., 2008) and Tbr1 (red) (which is expressed in layer VIa at perinatal ages; Hevner et al., 2001). While we did not detect a difference between control and mutant at E14.5 (A and B) or E15.5 (C and D), there was a noticeable difference in the distribution of *Sox6* mutant interneurons by P1 (E–H). *Sox6* mutant interneurons accumulate in layers I and VI at the expense of the more intermediate layers. This abnormal distribution persists at later times, with mutant *Sox6* interneurons preferentially occupying the superficial and deep cortical layers (layer I and VI, respectively), while being abnormally depleted in the intermediate cortical layers II–V (E–J). (I) The percentage of EGFP-expressing neurons in controls (black bars) and mutants (gray bars) in a given layer over the total number of EGFP in all layers at P17. Layer I: control (0.5% ± 0.3%) versus mutant (17% ± 6%), layer II/III: control (20% ± 3%) versus mutant (15% ± 3%), layer IV: control (16% ± 3%) versus mutant (5% ± 3%), layer V: control (31% ± 4%) versus mutant (22% ± 5%), and layer VI: control (28% ± 4%) versus mutant (36% ± 8%). (J) Total number of EGFP cells per optical field. Layer I: control (0.7 ± 0.6) versus mutant (22 ± 7), layer II/III: control (30 ± 6) versus mutant (18 ± 4), layer IV: control (24 ± 4) versus mutant (7 ± 3), layer V: control (49 ± 9) versus mutant (29 ± 5), layer VI: control (43 ± 11) versus mutant (49 ± 9), and total (I–VI): control (158 ± 15) versus mutant (130 ± 10). We analyzed three controls and three mutants at each of the time points examined: E14.5, E15.5, and P1. For the P17 analysis, we quantified the numbers of EGFP-expressing cells in the somatosensory corticies of fours pairs of controls/mutants. Arrow bars in (A) and (B) indicate blood vessels, which are labeled by the $Lhx6^{Cre}$ driver (Fogarty et al., 2007). Scale bar in (A) corresponds to 200 μm in (A)–(D) and 150 μm in (E)–(H).

cells at P17; Weiser et al., 1995) and Kv3.2 (normally expressed in PV-FS cells and some SST-expressing cells; Chow et al., 1999) was also accordingly decreased (Figures 5E–5G). Furthermore, in the remaining Kv3.2- and PV-positive neurons, the level of expression of these markers was strongly reduced. Moreover, 93% ± 6% of this population coexpressed NPY (Figure 4F). To ascertain the degree of cell death in conditional Sox6 mutants compared to that in control animals, we performed caspase 3 cleavage staining at E13.5, P1, and P17. At no age did we observe an obvious difference in apoptosis (results not shown). Consistent with this result, we observed that 93% ± 6% of the weakly PV-expressing cells displaced in layer I were NPY positive (compared to 4% ± 2% in control animals).

We also examined if there was any change in the number or location of non-MGE-derived interneurons (i.e., Lhx6-negative interneurons). This was accomplished in both control and conditional *Sox6* mutant animals by determining the number and location of EGFP-negative, VIP-expressing, and CR-expressing (SST-negative) interneurons. We observed no overall alteration in these interneuron subtypes in the absence of *Sox6* (Figure 5H).

NPY Is Upregulated Both Autonomously and Nonautonomously in Conditional *Sox6* Null Mutants

We observed that 23% ± 5% of the *Dlx5/6*-expressing population is NPY positive in control mice. However, when this population is examined in *Sox6* conditional null mice, 72% ± 7% of all interneurons express NPY. In addition, in both control and conditionally null mice, all NPY staining within the cortex is confined to interneurons (i.e., EGFP-expressing cells, Figures 4I and 4J). This observation allowed us to examine NPY expression in both MGE-derived and non-MGE-derived lineages by investigating the expression of NPY in $Sox6^{F/F};Lhx6^{Cre};RCE^{EGFP/+}$ animals (Figures 4C, 4D, 5C, 5G, and 5H). We reasoned that since NPY is confined to the interneuron population, all

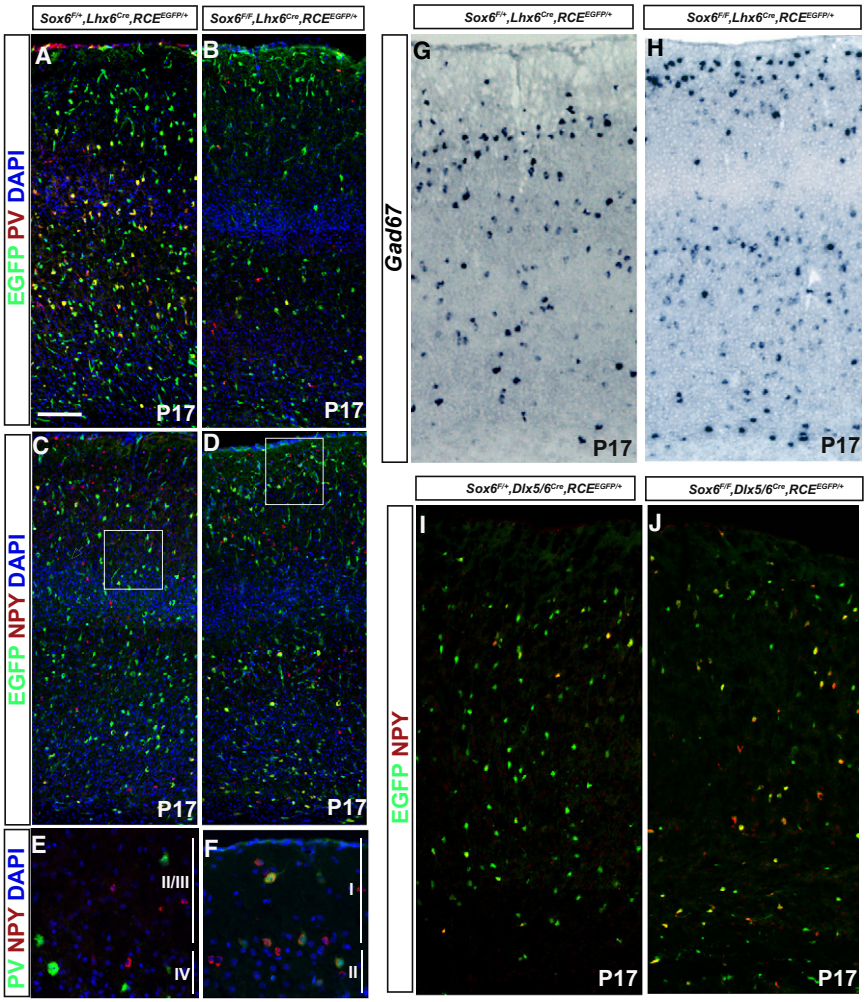

Figure 4. Effects of Loss of *Sox6* Gene Function on Cortical Interneuron Marker Expression

(A and B) Most of the *Sox6* mutant interneurons (*Sox6*$^{F/F}$;*Lhx6*^{Cre};*RCE*$^{EGFP/+}$) (green) lose PV (red) expression; however, a small percentage retain low levels of PV expression, some of which become ectopically positioned in layer I.

(C and D) In contrast, *Sox6* mutant interneurons upregulate NPY (red).

(E) In the control brains (*Sox6*$^{F/+}$;*Lhx6*^{Cre};*RCE*$^{EGFP/+}$), PV cells are distributed in layers II–VI (and absent in layer I), and a very low percentage of PV cells (green) coexpress NPY (red) (4% ± 2%).

(F) In contrast, in mutant brains (*Sox6*$^{F/F}$;*Lhx6*^{Cre};*RCE*$^{EGFP/+}$) some of the small amount of cells that exhibit low expression of PV are ectopically located in layer I. Virtually all the mutant PV-expressing cells (green) also express NPY (red) (93% ± 6%). (E) and (F) correspond to the squares in (C) and (D), respectively.

(G and H) *Gad67* expression was slightly decreased (19% ± 11%) in mutant animals (H).

(I and J) To determine if the upregulation of NPY is confined to the interneuron population, we performed NPY immunostaining (red) in *Dlx5/6* fate-mapped interneurons (pancortical interneuron marker) (green) in both (I) control (*Sox6*$^{F/+}$;*Dlx5/6*^{Cre};*RCE*$^{EGFP/+}$), and (H) mutant (*Sox6*$^{F/F}$;*Dlx5/6*^{Cre};*RCE*$^{EGFP/+}$) animals. We verified that the NPY upregulation in the mutant (J) is confined to the interneuron population (virtually all NPY-expressing cells double label for EGFP). Quantification of the percentage of NPY-expressing *Dlx5/6* fate-mapped interneurons shows a vast increase of NPY-expressing interneurons in the mutant (72% ± 7%) versus in the control (23% ± 5%). (I and J) The percentage was calculated as a total number of NPY-EGFP-expressing cells per total number of EGFP-expressing cells. We used a total of five animals for (A–F) and three for (G–J). Countings were performed in the somatosensory cortex at P17–P19.

Scale bar in (A) represents 70 μm in (A)–(D), 8 μm in (E)–(F), and 50 μm in (G)–(J).

NPY/EGP double-positive cells in the cortex of these mice must be MGE derived, while NPY-positive/EGFP-negative cells are not. NPY expression was strongly upregulated both autonomously (Figure 5G, 16% ± 2% in control versus 65% ± 4% in mutants; i.e. the percentage of EGFP-expressing cells that are NPY-positive) and nonautonomously (Figure 5H, 30% ± 3% in control versus 48% ± 5% in mutants; i.e. numbers of EGFP-negative/NPY-positive cells per area measured).

Sox6 Functions Genetically Downstream of *Lhx6*

The coexpression of Sox6 and Lhx6 within both the MGE and the postmitotic cortical interneurons derived from this structure is near complete. Moreover, *Lhx6* null mice resemble *Sox6* mutants in that MGE-derived cortical interneurons are similarly mispositioned, die at a comparable age, and are deficient in similar cortical interneuron populations (Liodis et al., 2007; Zhao et al., 2008). Taken together these facts suggest that within MGE progenitors, there exists a genetic interaction between *Lhx6* and *Sox6*. To test this hypothesis, we analyzed whether the reciprocal loss of *Lhx6* and *Sox6* within MGE-derived lineages effects the other's expression (Figure 6). At E15.5, in contrast to control neurons, MGE-derived *Lhx6* mutant interneurons rarely express Sox6, as assessed through Sox6 immunostaining of mice on a *Gad67*^{EGFP} (Tamamaki et al., 2003) background (Figures 6A and 6B). However, within the cortical VZ the expression of Sox6 was unperturbed (Figure 6B′).

To more specifically assess the genetic relationship between these two genes, we examined *Lhx6* heterozygote (*Lhx6*$^{+/-}$) and homozygote mutant (*Lhx6*$^{-/-}$) interneurons on a *Nkx2-1*^{Cre};*R26R*$^{YFP/+}$ background, which allowed us to directly visualize MGE-derived interneuron lineages independent of Lhx6 expression (Figures 6C and 6D). Using this approach, a similar result was obtained at both P2 (data not shown) and P15 (Figures 6C–6E). In Lhx6 mutant animals, we found that the vast majority of YFP-expressing cortical interneurons lose their expression of Sox6 (an 86% ± 4% decrease in the number of MGE

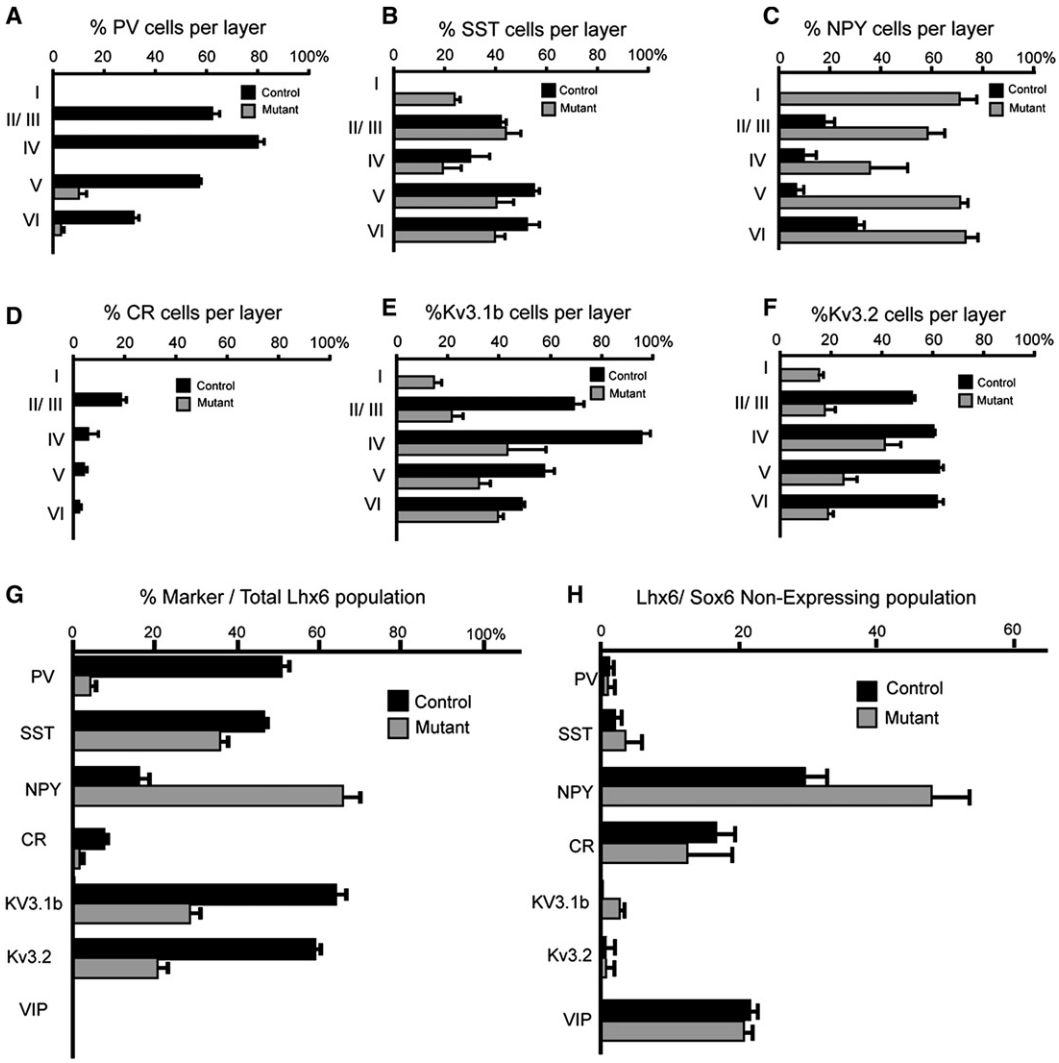

Figure 5. The Cell-Autonomous and Nonautonomous Affects Resulting from the Loss of *Sox6* Gene Function on Subtype-Specific Cortical Interneuron Marker Expression

(A–H) To determine which markers are affected in *Sox6* mutant cells, we compared control ($Sox6^{F/+};Lhx6^{Cre};RCE^{EGFP/+}$) (black bars) and mutant ($Sox6^{F/F};Lhx6^{Cre};RCE^{EGFP/+}$) (gray bars) animals at P17–P19. (A–F) The percentage of fate-mapped cells expressing a given marker relative to the total number of EGFP-positive neurons within that layer (marker-positive/EGFP-positive). The markers used were (A) parvalbumin (PV), (B) somatostatin (SST), (C) NPY, (D) calretinin (CR), (E) the voltage-sensitive potassium channel Kv3.1b, and (F) the voltage-sensitive potassium channel Kv3.2. (G) A summary of (A)–(F) showing the percentage of each marker examined, as a percentage of the total EGFP-positive cells within the somatosensory cortex (layer I–VI). Note that while the markers PV, SST, CR, Kv3.1b, and Kv3.2 are decreased, the marker NPY is increased. The extent to which individual markers are altered in the mutant differs in accordance with the layer examined (see A–F). (H) To determine the nonautonomous affects resulting from the loss of *Sox6* in non-MGE populations (i.e., those that are normally *Sox6*-negative) of cortical interneurons, we compared control ($Sox6^{F/+};Lhx6^{Cre};RCE^{EGFP/+}$) and mutant ($Sox6^{F/F};Lhx6^{Cre};RCE^{EGFP/+}$) mice for the expression of the analyzed markers within the EGFP-negative population. Values were calculated by counting the total number of marker and EGFP-negative cells per optical section. Note that the only marker affected in this analysis was NPY, which was significantly increased. All countings were performed at P17–P19. Bars correspond to stand error of the mean (n = 5).

fate-mapped interneurons expressing Sox6 in $Lhx6^{-/-}$ compared with $Lhx6^{+/-}$ animals). As noted above, in control animals we also observe a population of nonneural cortical cells that coexpress Sox6 and Olig2, and the proportion of these double-labeled cells was not affected in *Lhx6* mutants (Figures 6C and 6D).

In contrast, Lhx6 expression was not affected in *Sox6* mutants (85 ± 4 in controls and 78 ± 6 in mutant animals, per optical area examined; Figures 6F–6N). At E14.5, *Sox6* mutant cortical interneurons ($Dlx5/6^{Cre}$ fate-mapped EGFP-expressing cells) express *Lhx6* mRNA (Figures 6F and 6G) and Lhx6 protein (Figures 6H and 6I) comparably to that observed in control animals. Furthermore, these cells retain their Lhx6 expression at later ages (Figures 6L–6N). Taken together these results indicate that in MGE-derived cortical interneurons, although *Lhx6* is required for Sox6 expression, *Sox6* is not necessary for Lhx6

induction or maintenance. This leads us to conclude that *Sox6* functions genetically downstream of *Lhx6*.

Sox5 Does Not Compensate for the Loss of *Sox6* in Cortical Interneuron Lineages

Given the close homology between *Sox5* and *Sox6*, we were curious to determine whether any functional compensation by Sox5 occurs within cortical interneurons upon loss of *Sox6*. To address this issue specifically within the MGE-derived cortical interneuron populations, we examined whether the expression of Sox5 is cell-autonomously upregulated upon loss of *Sox6.* In these animals, Sox5 maintained a normal pattern of expression, and there was no indication that this protein is upregulated within the MGE-derived cortical interneuron population (Figures 6J and 6K and data not shown). This is distinct from the findings of a recent paper that shows that *Sox5* is upregulated in the *Sox6* null mouse (Azim et al., 2009). Taken together, these results suggest that at least within Lhx6 lineages, there is no evidence for compensation by Sox5 in *Sox6* conditional mutants, and hence the upregulation of *Sox5* in the absence of normal *Sox6* expression is not obligate.

We were also intrigued to explore the role of *Sox6* within the pallium. To specifically remove *Sox6* from cortical lineages, we bred the $Sox6^{F/F}$ conditional allele onto an $Emx1^{Cre}$ background (n = 3 for control and mutants). We investigated whether the loss of Sox6 in the pallium had an effect on P21 pyramidal neurons by examining the expression of SatB2 (Figures S2A and S2B), a marker for callosal projecting pyramidal neurons (Alcamo et al., 2008; Britanova et al., 2008), and Ctip2 (Figures S2C and S2D), expressed in corticofugal pyramidal neurons (Arlotta et al., 2005; Chen et al., 2008). In these mutants we saw no changes in these markers. To determine if the loss of this gene has a nonautonomous effect on cortical interneurons, we also examined these mutants for the expression of PV, SST, and NPY at P21 (Figures S2E–S2K). Neither analysis produced evidence that the loss of *Sox6* in the cortical primordium has an effect on cortical development. In addition, we did not observe any overt behavioral phenotype or seizures in these animals (results not shown).

Sox6 Mutant FS Basket Cells Exhibit Immature Intrinsic Properties

The loss of Sox6 results in the ectopic positioning of Lhx6-lineage cells to the periphery of the cortical plate, and to layer I in particular. This provided us with the unique opportunity to record the electrophysiological properties of cells of known subtypes within layers where they do not normally reside. The Lhx6 lineage includes all MGE-derived cortical interneurons, and is largely composed of two main subgroups that express SST and PV. The latter group contains a rather homogenous population of basket cell interneurons characterized as FS. Although PV is lost in the majority of *Sox6* mutant interneurons (Figures 4 and 5), SST expression is less affected. We performed whole-cell current-clamp recordings of EGFP-labeled cells in layer I of acute brain slices from P14–P16 mice, with subsequent post hoc immunohistochemistry for SST and Kv3.1b. All cells (n = 4) that proved to be negative for SST possessed a firing pattern that clearly resembled that of wild-type FS interneurons. Kv3.1b expression in these cells, while present, was strongly reduced compared to that of controls (Figures 7A and 7B). The dendritic arbors of these cells were large and highly arborized, and the axons formed the typical "baskets" around the cell somas of neighboring cells (Figure 7C), suggesting that they are relatively mature. In order to assay the maturity and integration of the mutant cells in greater detail, we compared their electrophysiological properties to those of FS cells in layer II/III of control animals (Figures 7D–7G and Table S1; n = 3).

The mutant cells were indistinguishable from the control cells with regards to passive membrane properties, such as resting membrane potential (RMP), input resistance (R_{in}), and membrane constant tau (See Table S1). Similarly, the spike and after-hyperpolarization (AHP) kinetics, such as half-spike width, AHP time to the lowest point, and AHP amplitude were not significantly different. However, the multiple spike dynamics of the mutant cells had a lower max firing rate and a more pronounced intraspike interval (ISI) adaptation (Figure 7E; $p = 0.047$ and $p = 0.0004$, respectively), and were unable to sustain firing during prolonged (5 s) protocols (Figure 7F). Furthermore, mutant cells exhibited a higher firing threshold (Figure 7E; $p = 0.019$) and more pronounced sag (7.1 ± 1.5 mV versus 2.9 ± 1.9 mV; $p = 0.020$) during hyperpolarizing steps, collectively suggesting that these cells are retarded in their maturation (Itami et al., 2007; Okaty et al., 2009).

A characteristic of the immature cortex is that the frequency of EPSPs in FS basket cells increases dramatically during development between P10 and P14 (Okaty et al., 2009). To test whether the ectopically positioned FS interneuron population received normal levels of excitatory input, we held the cells at −72 mV for at least 2 min and measured the frequency at which they received excitatory input. Perhaps surprisingly, there was no difference between the mutant ectopic cells and the control layer II/III FS cells (Figure 7G). In conclusion, while the mutant cells have normal morphology and receive appropriate levels of input, their electrophysiological properties suggest that FS cell maturation is impaired.

Removal of Sox6 in MGE-Derived Lineages Leads to a Severe Epileptic Encephalopathy

Sox6 mutants were undistinguishable from their littermates until approximately 15 days of age, at which point they developed spasticity, as evidenced by an abnormal scissoring posture of the limbs when mutants were held by the tail. By P16, they became progressively more withdrawn and developed spontaneous seizures. They died between P17 and P19 of a combination of prolonged seizures and dehydration.

To further assess the seizure phenotype, four mutants (two $Sox6^{F/F}$;$Dlx5/6^{Cre}$ and two $Sox6^{F/F}$;$Lhx6^{Cre}$ were combined as they had indistinguishable phenotypes) and four wild-type controls were monitored daily by video electroencephalography (EEG) from P16.

The epileptic phenotype was found to be temporally progressive in all recorded mutants. During early P16, mutants remained able to explore and presented minimal cortical EEG anomalies. They were able to generate background theta rhythms similarly to controls, although these were somewhat less well sustained

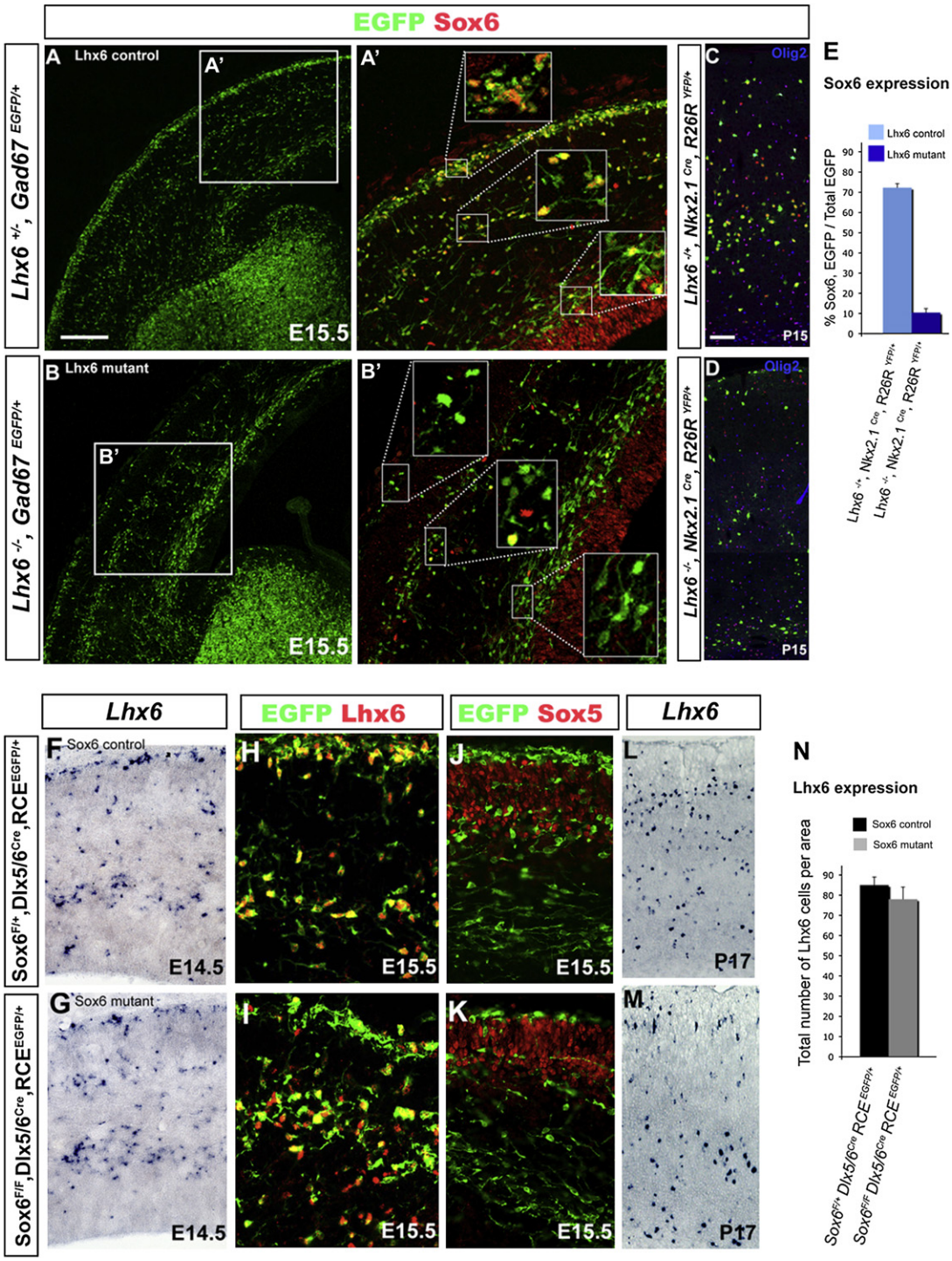

Figure 6. *Sox6* Is Genetically Downstream of *Lhx6*

To test the genetic relationship between *Sox6* and *Lhx6*, we analyzed the expression of both Sox6 in *Lhx6* mutants (A–E), and Lhx6 in *Sox6* mutants (F–N). Sox6 expression is dramatically decreased in *Lhx6* mutant mice ($Lhx6^{-/-}$) at both E15.5 (A and B) and P15 (C and D). (A) In E15.5 control mice ($Lhx6^{+/-}$, $Gad6^{EGFP}$), migrating cortical interneurons (green) express Sox6 (red), and this expression is dramatically decreased in mutant ($Lhx6^{-/-}$, $Gad6^{EGFP}$) mice (B). By contrast, Sox6 cortical VZ expression is not affected in the *Lhx6* mutant. (C and D) A decrease of Sox6 in *Lhx6* mutant interneurons is still observed at P15. In order to test the extent of the Sox6 decrease in *Lhx6* mutant interneurons, we fate-mapped MGE-derived interneurons (green) by examining both (C) control ($Lhx6^{+/-}$;$Nkx2\text{-}1^{Cre}$;$R26R^{YFP/+}$) and (D) mutant ($Lhx6^{-/-}$;$Nkx2\text{-}1^{Cre}$;$R26R^{YFP/+}$) alleles with the $Nkx2\text{-}1^{Cre}$ driver. There was an obvious decrease in the expression of Sox6 in *Nkx2-1* fate-mapped *Lhx6* mutant cells, while there was no change in Sox6 expression in Olig2-expressing nonneural cells (blue). (E) The percentage of Sox6-expressing interneurons in the fate-mapped Nkx2-1 lineage was calculated as the ratio between the number of cells that are Sox6 positive/YFP positive, in

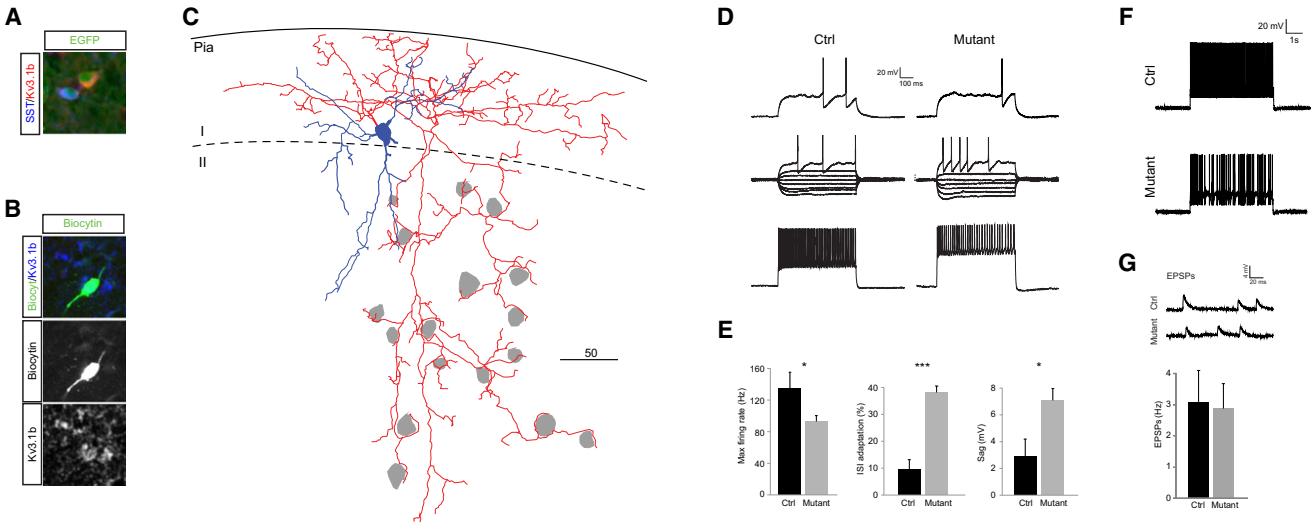

Figure 7. Physiological Characterization of Ectopic Fast-Spiking Cells in Layer I

(A) Nonoverlapping MGE-derived populations in layer I express SST and Kv3.1b.

(B) Post hoc immunostaining for Kv3.1b in a recorded SST-negative FS basket cell.

(C) Neurolucida reconstruction of a recorded cell reveals a relatively mature morphology and that the ectopic cells retain the typical innervation of cell somas (in gray).

(D–F) Intrinsic properties associated with maturation are abnormal in *Sox6* mutants. (D) Representative traces from the 500 ms protocol used from layer I mutant cells compared to a layer II/III control FS cell. (E) Significantly lower F_{max} ($p = 0.047$), higher ISI adaptation ($p = 0.0004$), and larger sag ($p = 0.020$) suggest a less mature phenotype. (F) The mutant cells fails to maintain a high-frequency firing rate during a prolonged 5 s protocol.

(G) The frequency of EPSPs is similar in *Sox6* mutants and control littermates.

and repeatedly intertwined with slower delta waves (Figure 8A). Already at P16, the interictal trace revealed bilateral synchronous bursts of epileptic activity in the hippocampi characterized by fast polyspikes overlying high-amplitude delta waves. This epileptic anomaly was accentuated during slow-wave sleep (Figure 8B) and was occasionally accompanied by cortical delta waves or polyspikes, behaviorally manifested as slowing or rapid axial myoclonus (Figure 8C). Within the next 24 hr, mutants developed generalized seizures (Figure 8D) manifested as an initial axial myoclonus followed by intermittent fine limb and axial clonus. Epileptic activity during these seizures was most often confined to the cortex, with intermittent recruitment of the hippocampi.

Spectral analysis performed on slow-wave sleep epochs at late P16.5 and early P17 illustrated the interictal anomalies described above. Examination of the cortical EEG (M1) revealed increased spectral amplitude in the delta frequency band (228 μV/Hz in mutants versus 163 μV/Hz in controls, n = 4). In addition, epileptic bursts observed in the hippocampi were reflected in spectral analyses as increased spectral amplitude in the delta frequency band (Figure 9B, 292 μV/Hz in mutants versus 199 μV/Hz in controls), as well as in the beta (43 μV/Hz versus 30.8 μV/Hz) and gamma (28 μV/Hz versus 17 μV/Hz) frequency bands (Figures 9A and 9C). Notably, the spectral amplitude estimates in CA1 revealed a significant new peak around 25 ± 3 Hz in the beta range with a minor peak around 53 ± 3 Hz in the gamma range (Figure 9A).

DISCUSSION

In the present study, we describe the role of *Sox6* in cortical interneuron development, and the consequences of its removal, from a cellular to a behavioral level. We identify Sox6 as a protein expressed continuously within MGE-derived cortical interneurons from postmitotic progenitors into adulthood. Both its expression pattern and null phenotype suggests that *Sox6* gene function is closely related to that of *Lhx6.* The two genes appear to be largely coexpressed in MGE-derived interneuron lineages (Figures 1C and 1D). Moreover, in both *Lhx6* and *Sox6* null animals, the expression of PV basket cells and SST Martinotti neurons is abnormal. Examination of the genetic relationship between these two genes led us to conclude that Sox6 functions downstream of *Lhx6* (Figure 6). Electrophysiological analysis of *Sox6* mutant cortical interneurons revealed that basket cells, even when mispositioned, retain characteristic but immature

either Lhx6 control (72% ± 2% in $Lhx6^{+/-};Nkx2\text{-}1^{Cre};R26R^{YFP/+}$) or mutant (10% ± 2% in $Lhx6^{-/-};Nkx2\text{-}1^{Cre};R26R^{YFP/+}$) mice. (F–N) Lhx6 expression is not affected in *Sox6* mutant cells. (F–I) We saw no difference between E14.5 controls ($Sox6^{F/+};Dlx5/6^{Cre};RCE^{EGFP/+}$) and mutants ($Sox6^{F/F};Dlx5/6^{Cre};RCE^{EGFP/+}$) in *Lhx6*/Lhx6 expression as assessed by in situ staining (F and G) and antibody staining (H and I). Similarly, we saw no difference in the expression of Sox5 (red) in control versus mutant mice (J and K). (L and N) *Lhx6* expression was still largely unaltered at P17. (N) *Lhx6* expression was calculated as the total number of *Lhx6*-expressing cells at P17 in both the control (85% ± 4% in $Sox6^{F/+};Dlx5/6^{Cre};RCE^{EGFP/+}$) and mutant (78% ± 6% in $Sox6^{F/F};Dlx5/6^{Cre};RCE^{EGFP/+}$) mice. Scale bar in (A) corresponds to 300 μm in (A) and (B). Scale bar in (C) corresponds to 50 μm in (C) and (D), 25 μm in (F)–(J), and 40 μm in (L) and (M).

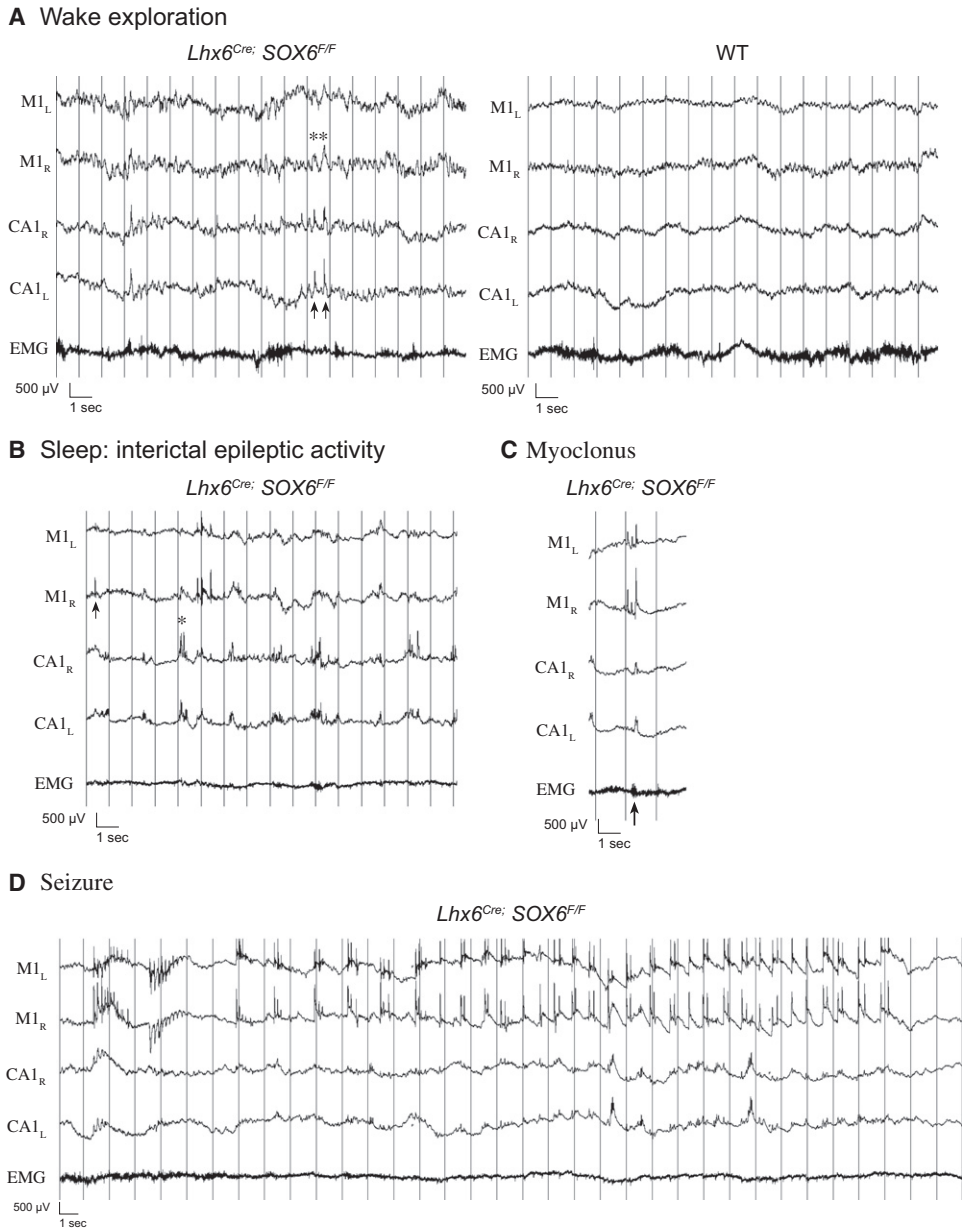

Figure 8. EEG Characterization

(A) Mutant P16 EEG recordings in cortical fields (M1) reveal dysrhythmic theta oscillations interrupted by high-amplitude delta waves (asterisk) often associated with hippocampal epileptic discharges in CA1 (arrows).

(B) Interrictal epileptic activity becomes more prominent during slow-wave sleep with independent discharges in the cortex (arrow) and hippocampi (asterisk).

(C) Although usually asymptomatic and considered interictal, simultaneous epileptic discharges in the hippocampi and polyspike complexes in the cortex occasionally manifest as generalized myoclonus.

(D) Generalized seizures with synchronous bifrontal onset often remain confined to cortical fields, with variable hippocampal involvement.

Acquisition: 2000 Hz, HP 0.1 Hz, LP 300 Hz, filtered at LP 70 Hz for display.

FS physiological features (Figure 8). Taken together, our data suggest that Sox6 is not required for the specification or maintenance of MGE-derived cortical interneuron subtypes. It is, however, necessary for their normal positioning and maturation. As a consequence, the specific removal of *Sox6* from this population results in severe epileptic encephalopathy.

The Autonomous and Nonautonomous Requirements for *Sox6* in Cortical Interneuron Lineages

In the straight *Sox6* null mutant, we and others (Azim et al., 2009) observed a dramatic loss of PV and SST expression and a concomitant increase in NPY expression. Based on our previous analysis of *Nkx2-1* (Butt et al., 2008), we initially surmised that

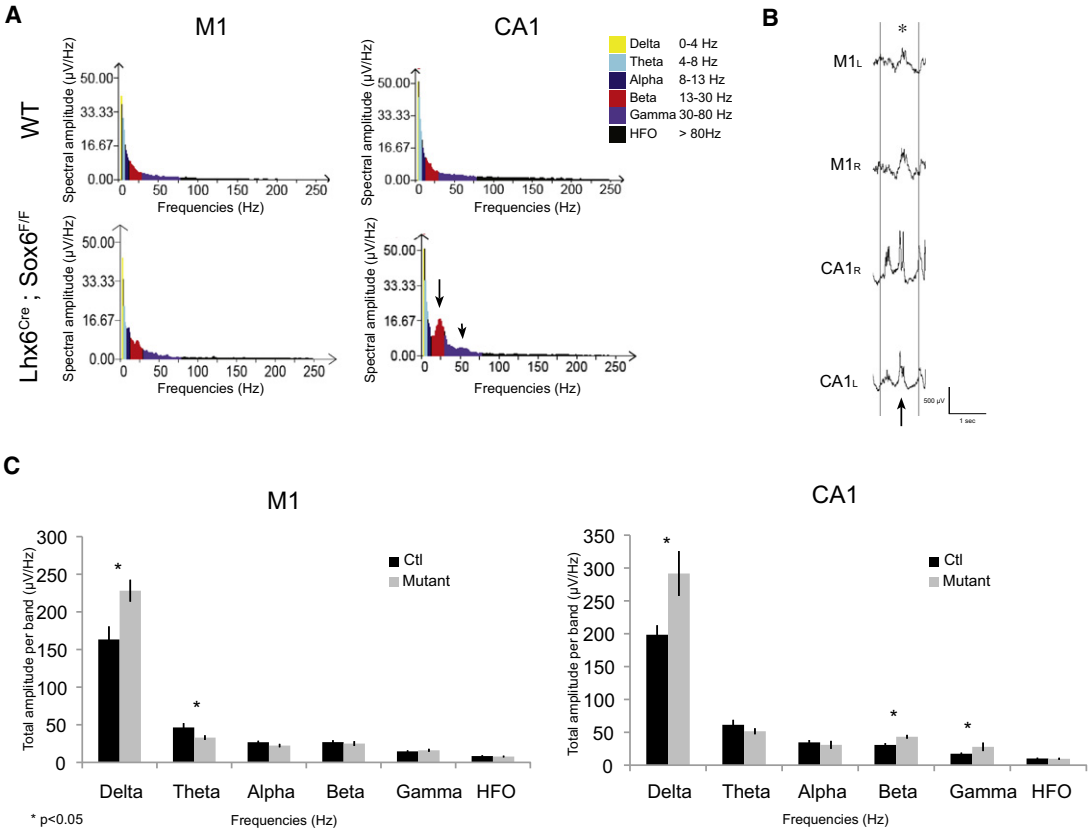

Figure 9. Spectral Analysis

Spectral analysis during slow-wave sleep at P17 ±0.5D (FFT 1 s, average of six 10 s epochs) is illustrated here as (A) representative individual spectra and (C) total spectral amplitude per frequency band (with standard error). Analysis reveals spectral band amplitude (square root power) modifications with increased delta power band and decreased theta power band in cortical EEG (A and C) reflecting frequent high-amplitude delta waves (B, asterisk). In addition, delta, beta, and gamma powers were increased in hippocampal recordings (A arrow, C: additional peaks at 25.5 ± 0.5 Hz and minor peak at 53 ± 3 Hz, reflecting frequent epileptic bursts composed of high-amplitude delta waves with superimposed polyspikes (B, arrow).

this result indicated a "class-switching" of PV and SST cells into a NPY subtype. Indeed, this is the conclusion reached by the Macklis group in their recent analysis (Azim et al., 2009). However, our analysis of the NPY-expressing ectopic cells in layer I revealed that they possess low levels of PV and Kv3.1b expression and retain FS physiological character, arguing against such a fate-switch. Furthermore, our finding that NPY is also upregulated in cells that have not lost *Sox6* expression suggests that the expression of this protein is related more to an ambient increase in cortical activity in these seizure-prone animals than as a marker of interneuron subtype. Indeed, it is known that *NPY* mRNA expression is increased in response to neuronal activity (Baraban et al., 1997; Nawa et al., 1995), consistent with the presence of this protein in a variety of cortical interneuron subtypes (Karagiannis et al., 2009). Hence, we hypothesize that the upregulation in NPY expression that we observe in these mutants may be secondary to the increase in cortical activity that ultimately manifests itself in seizures.

The Genetic Relationship between *Sox6* and *Lhx6*

Sox6 has been most noted for its requirement in bone and oligodendrocyte development (Smits et al., 2001; Stolt et al., 2006) while *Lhx6* is involved in the formation of limbic circuitry (Choi et al., 2005). Despite these divergent roles, their functions appear tightly linked within MGE-derived cortical interneuron lineages. The onset of expression of both these genes appears to be dependent on *Nkx2-1* (Du et al., 2008; data not shown; Figures 1D and 1D′). Although the expression of SST appears more severely affected in *Lhx6* null mice, the removal of either gene results in a similar loss of markers and mispositioning of interneurons.

Based on our observations that Lhx6 expression persists in *Sox6* mutants while Sox6 expression is lost in *Lhx6* mutants, it seems likely that *Lhx6* functions genetically upstream of *Sox6.* It is however not known whether *Lhx6* directly binds to the promoter of *Sox6*. Within the embryo as a whole, the colocalization of *Lhx6* and *Sox6* is the exception rather than the rule, as outside the telencephalon *Lhx6* and *Sox6* are found in different tissues. Hence, a direct transcriptional relationship must require ancillary partners for *Lhx6* to initiate *Sox6* expression. Alternatively, Lhx6 and Sox6 proteins might physically interact to form a transcription complex that fails to function if either partner is absent. If so, Lhx6 would be posited to both initiate Sox6 expression and subsequently interact functionally with it. Furthermore,

given the similarity in their loss-of-function phenotypes, one might construe that the absence of Sox6 in *Lhx6* mutants accounts for much of the defects observed. In future experiments it will be interesting to gain a more fine-grained understanding of the relative requirement for these two genes in cortical interneuron development.

The Physiological and Behavioral Consequences of *Sox6* Removal

The epileptic phenotype observed upon conditional removal of *Sox6* resembles other mutants in which MGE-derived interneurons are abnormal, including *Nkx2-1* and *Lhx6* null mice, which also develop spontaneous seizures (Butt et al., 2008). However, the temporal emergence of these anomalies and the relative contribution of the hippocampus and the cortex to seizure development have not been previously evaluated.

These mutants appeared phenotypically normal until P15, revealing that intact MGE-derived interneurons are not initially required for the normal development of animal behavior. However, they subsequently developed a severe seizure disorder. Interestingly, cortical excitatory synaptic inputs normally reach their maximal level at P15 (Okaty et al., 2009). This network activity coincides with developmental changes in PV-expressing FS interneurons during the third and fourth postnatal week, including the maturation of their intrinsic cell firing properties, the development of perineural nets, and an improved reliability of GABA release (Doischer et al., 2008; Okaty et al., 2009). In our analysis, the ectopically located neurons displayed intrinsic physiological characteristics of less mature FS cells, including an inability to sustain fast firing, greater ISI adaptation, and a lack of both perineural nets (data not shown) and PV expression. These two latter properties of FS cells are crucial in regulating plasticity within the cortex (Pizzorusso et al., 2002; Sugiyama et al., 2008). Specifically, adequate expression of PV has been shown to play an important role in presynaptic calcium homeostasis and neurotransmitter production and release (Caillard et al., 2000; Rutherford et al., 1997).

At present we cannot definitely say whether the apparent immaturity of the cells is caused by intrinsic genetic changes due to the lack of Sox6, or is due to their mispositioning. The fact that even those cells that are correctly positioned in layer II/III and IV lack PV expression argues that some of the cellular phenotype is caused by cell-intrinsic loss of Sox6. Nevertheless, these findings suggest that correctly located FS basket cells become crucial in dampening excitation and preventing seizures during the third postnatal week. It is interesting to note that a similar pattern of normal early development followed by abrupt onset of seizures is observed in children with catastrophic childhood epilepsies (Nabbout and Dulac, 2003).

Combined Contribution of Hippocampus and Cortex to the Epileptic Phenotype

Our analysis reveals that epileptic activity appears in the hippocampus prior to the cortex as early as P16. This is consistent with earlier maturation of hippocampal basket cells (P11) compared to their cortical counterparts (P15–P19) (Nabbout and Dulac, 2003; Okaty et al., 2009). Although minimally symptomatic, this sparse hippocampal epileptic activity may contribute to the induction of persistent epileptic circuits in the hippocampus and possibly efferent cortical areas (Ben-Ari, 2006). However, it is remarkable that *Sox6* mutants become significantly more symptomatic after independent epileptic activity appears in the cortex, suggesting it may be largely responsible for the severity of the observed epileptic encephalopathy.

The precise contribution of FS basket cells to various cortical oscillations is still being investigated (Bartos et al., 2007; Cardin et al., 2009; Sohal et al., 2009; Wulff et al., 2009). Our analysis reveals that despite gross anomalies in the development of MGE-derived interneuron populations, *Sox6* conditional mutants are able to generate rhythms in all frequency bands. FS basket cells are thought to play an important role in the generation and timing of gamma oscillations (Buhl et al., 2003; Cardin et al., 2009; Hormuzdi et al., 2001; Sohal et al., 2009; Traub et al., 1996, 1997). Nevertheless, gamma oscillations were generated in *Sox6* mutants and particularly increased during epileptic discharges in the hippocampus. Similar rhythms have been reported during seizures in PV knockout mice and kainite-induced hippocampal seizures (Medvedev et al., 2000; Schwaller et al., 2004). Moreover, FS basket cells are known to contribute to finer properties of the gamma oscillations in a task-specific manner (Fries et al., 2001; Montgomery et al., 2008; Popa et al., 2009). It will thus be interesting to evaluate how these rhythms are modified in *Sox6* conditional mutants when elicited during more specific tasks in the awake, behaving animal.

EXPERIMENTAL PROCEDURES

Animal Handling

All animal handling and maintenance was performed according to the regulations of the Institutional Animal Care and Use Committee of the NYU School of Medicine. The *Dlx5/6*^{Cre} (Stenman et al., 2003), *Lhx6*^{Cre} (Fogarty et al., 2007), *Nkx2.1*^{Cre} (Fogarty et al., 2007), *Sox6*$^{F/+}$ (Dumitriu et al., 2006), *Lhx6*$^{-/+}$ (Liodis et al., 2007), *RCE*$^{EGFP/+}$ (note that the original name of this line is *RCE:loxP*; Sousa et al., 2009), *Gad67*^{EGFP} (Tamamaki et al., 2003), *Emx1*^{Cre} (Iwasato et al., 2004), and *R26R*$^{YFP/+}$ (Srinivas et al., 2001) transgenic lines were maintained in a mixed background (Swiss Webster and C57/B16) and genotyped as previously described (Butt et al., 2008; Dumitriu et al., 2006; Fogarty et al., 2007; Srinivas et al., 2001; Stenman et al., 2003).

In Vivo *Sox6* Conditional Loss of Function and Fate-Mapping of Cortical Interneurons

Male *Sox6*$^{F/+}$;*Dlx5/6*^{Cre} or *Sox6*$^{F/+}$;*Lhx6*^{Cre} mice were crossed to *Sox6*$^{F/F}$;*RCE*$^{EGFP/EGFP}$ females to generate productive *Sox6*$^{F/+}$;*Dlx5/6*^{Cre};*RCE*$^{EGFP/+}$ (control); *Sox6*$^{F/F}$;*Dlx5/6*^{Cre};*RCE*$^{EGFP/+}$ (mutant); or *Sox6*$^{F/+}$;*Lhx6*^{Cre};*RCE*$^{EGFP/+}$ (control); *Sox6*$^{F/F}$;*Lhx6*^{Cre};*RCE*$^{EGFP/+}$ (mutant) offspring. Our entire analysis was based on examination of outbred mice. Indeed, preliminary examination of the phenotype resulting from the loss of *Sox6* gene function on mice maintained on a Black 6 inbred background indicated that these animals suffer from a phenotype more severe than that which we observed in our analysis of outbred mice.

Histology and Cell Counting

See the Supplemental Data for the details of these methods.

Acute In Vitro Cortical Slice Electrophysiology and Morphological Reconstruction

Whole-cell patch-clamp electrophysiological recordings were performed on EGFP-expressing cells in acute brain slices prepared from P14–P16 animals,

as previously described (Miyoshi et al., 2007b), with the exception that biocytin, instead of Lucifer yellow, was used in the intracellular solution for filling the cells. For details on these methods and the analysis of intrinsic properties and EPSPs see the Supplemental Data.

EEG Video Monitoring

Animals were recorded daily starting at P16 in 3 hr sessions, once or twice daily, and were returned to their home cage between recording sessions. Electroencephalographic signal was acquired at 2000 Hz acquisition speed, filtered at HP 0.1 Hz and LP 300 Hz, and digitalized using Stellate Harmonie acquisition system with simultaneous video monitoring. Traces were analyzed subsequently and spectral analysis was completed using Stellate Harmony EEG software. Spectral analysis was carried out using Stellate Harmony Spectrum software. Artifact-free interictal EEG segments during slow-wave sleep (defined as prominence of delta waves on cortical EEG recording with absence of movement confirmed by EMG and video) were analyzed using Fast-Fourrier transformation (FFT 1 s, average of 60 segments), and mean root power (signal amplitude) for each spectral band (as defined in Figure 9A) were compared between mutants and controls. For further details see the Supplemental Data.

SUPPLEMENTAL DATA

Supplemental data for this article include Supplemental Experimental Procedures, two figures, and a table and can be found at http://www.cell.com/neuron/supplemental/S0896-6273(09)00590-X.

ACKNOWLEDGMENTS

Research in the Fishell laboratory is supported by R01MH068469 and R01NS039007 Grants from the NIMH and the NINDS, respectively, as well as generous support from the Simons Foundation. R.B. was funded by Fundacao Ciencia e Tecnologia (FCT). E.R. is funded by the Quebec Health Research Fund (FRSQ). J.H.L. was funded by the Swedish Brain Foundation (Hjärnfonden) postdoctoral grant and is currently an EMBO long-term fellow. We wish to thank Dr. Nicoletta Kessaris for providing the *Lhx6*^{Cre} and *Nkx2-1*^{Cre} mouse lines; Frank Costatini for providing the *R26R*^{YFP} line; Takuji Iwasato for his *Emx1*^{Cre}; and Yuchio Yanagawa for his generous gift of his *Gad67*^{EGFP} allele. We would like to thank Bernardo Rudy for the generous gift of the antibodies Kv3.1b and Kv3.2. We would also like to thank Lihong Yin for excellent technical help. We thank members of the Fishell laboratory for critically reading this manuscript. We would also like to thank Goichi Miyoshi for generously sharing with us unpublished results.

Accepted: August 14, 2009
Published: August 26, 2009

REFERENCES

Alcamo, E.A., Chirivella, L., Dautzenberg, M., Dobreva, G., Fariñas, I., Grosschedl, R., and McConnell, S.K. (2008). Satb2 regulates callosal projection neuron identity in the developing cerebral cortex. Neuron *57*, 364–377.

Alifragis, P., Liapi, A., and Parnavelas, J.G. (2004). Lhx6 regulates the migration of cortical interneurons from the ventral telencephalon but does not specify their GABA phenotype. J. Neurosci. *24*, 5643–5648.

Allene, C., Cattani, A., Ackman, J.B., Bonifazi, P., Aniksztejn, L., Ben-Ari, Y., and Cossart, R. (2008). Sequential generation of two distinct synapse-driven network patterns in developing neocortex. J. Neurosci. *28*, 12851–12863.

Anderson, S.A., Eisenstat, D.D., Shi, L., and Rubenstein, J.L. (1997a). Interneuron migration from basal forebrain to neocortex: dependence on Dlx genes. Science *278*, 474–476.

Anderson, S.A., Qiu, M., Bulfone, A., Eisenstat, D.D., Meneses, J., Pedersen, R., and Rubenstein, J.L. (1997b). Mutations of the homeobox genes Dlx-1 and Dlx-2 disrupt the striatal subventricular zone and differentiation of late born striatal neurons. Neuron *19*, 27–37.

Anderson, S.A., Marin, O., Horn, C., Jennings, K., and Rubenstein, J.L. (2001). Distinct cortical migrations from the medial and lateral ganglionic eminences. Development *128*, 353–363.

Ang, E.S., Jr., Haydar, T.F., Gluncic, V., and Rakic, P. (2003). Four-dimensional migratory coordinates of GABAergic interneurons in the developing mouse cortex. J. Neurosci. *23*, 5805–5815.

Arlotta, P., Molyneaux, B.J., Chen, J., Inoue, J., Kominami, R., and Macklis, J.D. (2005). Neuronal subtype-specific genes that control corticospinal motor neuron development in vivo. Neuron *45*, 207–221.

Azim, E., Jabaudon, D., Fame, R.M., and Macklis, J.D. (2009). SOX6 controls dorsal progenitor identity and interneuron diversity during neocortical development. Nat. Neurosci., in press. Published online August 5, 2009. 10.1038/nn.2387.

Baraban, S.C., Hollopeter, G., Erickson, J.C., Schwartzkroin, P.A., and Palmiter, R.D. (1997). Knock-out mice reveal a critical antiepileptic role for neuropeptide Y. J. Neurosci. *17*, 8927–8936.

Bartos, M., Vida, I., and Jonas, P. (2007). Synaptic mechanisms of synchronized gamma oscillations in inhibitory interneuron networks. Nat. Rev. Neurosci. *8*, 45–56.

Batista-Brito, R., Machold, R., Klein, C., and Fishell, G. (2009). Gene expression in cortical interneuron precursors is prescient of their mature function. Cereb. Cortex *18*, 2306–2317.

Ben-Ari, Y. (2006). Basic developmental rules and their implications for epilepsy in the immature brain. Epileptic Disord. *8*, 91–102.

Britanova, O., de Juan Romero, C., Cheung, A., Kwan, K.Y., Schwark, M., Gyorgy, A., Vogel, T., Akopov, S., Mitkovski, M., Agoston, D., et al. (2008). Satb2 is a postmitotic determinant for upper-layer neuron specification in the neocortex. Neuron *57*, 378–392.

Buhl, D.L., Harris, K.D., Hormuzdi, S.G., Monyer, H., and Buzsaki, G. (2003). Selective impairment of hippocampal gamma oscillations in connexin-36 knock-out mouse in vivo. J. Neurosci. *23*, 1013–1018.

Butt, S.J., Fuccillo, M., Nery, S., Noctor, S., Kriegstein, A., Corbin, J.G., and Fishell, G. (2005). The temporal and spatial origins of cortical interneurons predict their physiological subtype. Neuron *48*, 591–604.

Butt, S.J., Sousa, V.H., Fuccillo, M.V., Hjerling-Leffler, J., Miyoshi, G., Kimura, S., and Fishell, G. (2008). The requirement of Nkx2-1 in the temporal specification of cortical interneuron subtypes. Neuron *59*, 722–732.

Caillard, O., Moreno, H., Schwaller, B., Llano, I., Celio, M.R., and Marty, A. (2000). Role of the calcium-binding protein parvalbumin in short-term synaptic plasticity. Proc. Natl. Acad. Sci. USA *97*, 13372–13377.

Cardin, J.A., Carlen, M., Meletis, K., Knoblich, U., Zhang, F., Deisseroth, K., Tsai, L.H., and Moore, C.I. (2009). Driving fast-spiking cells induces gamma rhythm and controls sensory responses. Nature *459*, 663–667.

Chen, B., Wang, S.S., Hattox, A.M., Rayburn, H., Nelson, S.B., and McConnell, S.K. (2008). The Fezf2-Ctip2 genetic pathway regulates the fate choice of subcortical projection neurons in the developing cerebral cortex. Proc. Natl. Acad. Sci. USA *105*, 11382–11387.

Choi, G.B., Dong, H.W., Murphy, A.J., Valenzuela, D.M., Yancopoulos, G.D., Swanson, L.W., and Anderson, D.J. (2005). Lhx6 delineates a pathway mediating innate reproductive behaviors from the amygdala to the hypothalamus. Neuron *46*, 647–660.

Chow, A., Erisir, A., Farb, C., Nadal, M.S., Ozaita, A., Lau, D., Welker, E., and Rudy, B. (1999). K(+) channel expression distinguishes subpopulations of parvalbumin- and somatostatin-containing neocortical interneurons. J. Neurosci. *19*, 9332–9345.

Cobos, I., Calcagnotto, M.E., Vilaythong, A.J., Thwin, M.T., Noebels, J.L., Baraban, S.C., and Rubenstein, J.L. (2005). Mice lacking Dlx1 show subtype-specific loss of interneurons, reduced inhibition and epilepsy. Nat. Neurosci. *8*, 1059–1068.

Cobos, I., Long, J.E., Thwin, M.T., and Rubenstein, J.L. (2006). Cellular patterns of transcription factor expression in developing cortical interneurons. Cereb. Cortex *16* (*Suppl 1*), i82–i88.

Corbin, J.G., Gaiano, N., Machold, R.P., Langston, A., and Fishell, G. (2000). The Gsh2 homeodomain gene controls multiple aspects of telencephalic development. Development *127*, 5007–5020.

Corbin, J.G., Nery, S., and Fishell, G. (2001). Telencephalic cells take a tangent: non-radial migration in the mammalian forebrain. Nat. Neurosci. *4* (*Suppl*), 1177–1182.

Doischer, D., Hosp, J.A., Yanagawa, Y., Obata, K., Jonas, P., Vida, I., and Bartos, M. (2008). Postnatal differentiation of basket cells from slow to fast signaling devices. J. Neurosci. *28*, 12956–12968.

Du, T., Xu, Q., Ocbina, P.J., and Anderson, S.A. (2008). NKX2-1 specifies cortical interneuron fate by activating Lhx6. Development *135*, 1559–1567.

Dumitriu, B., Dy, P., Smits, P., and Lefebvre, V. (2006). Generation of mice harboring a Sox6 conditional null allele. Genesis *44*, 219–224.

Fogarty, M., Grist, M., Gelman, D., Marin, O., Pachnis, V., and Kessaris, N. (2007). Spatial genetic patterning of the embryonic neuroepithelium generates GABAergic interneuron diversity in the adult cortex. J. Neurosci. *27*, 10935–10946.

Fragkouli, A., Hearn, C., Errington, M., Cooke, S., Grigoriou, M., Bliss, T., Stylianopoulou, F., and Pachnis, V. (2005). Loss of forebrain cholinergic neurons and impairment in spatial learning and memory in LHX7-deficient mice. Eur. J. Neurosci. *21*, 2923–2938.

Fries, P., Reynolds, J.H., Rorie, A.E., and Desimone, R. (2001). Modulation of oscillatory neuronal synchronization by selective visual attention. Science *291*, 1560–1563.

Gelman, D.M., Martini, F.J., Nóbrega-Pereira, S., Pierani, A., Kessaris, N., and Marín, O. (2009). The embryonic preoptic area is a novel source of cortical GABAergic interneurons. J. Neurosci. *29*, 9380–9389.

Ghanem, N., Yu, M., Long, J., Hatch, G., Rubenstein, J.L., and Ekker, M. (2007). Distinct cis-regulatory elements from the Dlx1/Dlx2 locus mark different progenitor cell populations in the ganglionic eminences and different subtypes of adult cortical interneurons. J. Neurosci. *27*, 5012–5022.

Glickfeld, L.L., Roberts, J.D., Somogyi, P., and Scanziani, M. (2009). Interneurons hyperpolarize pyramidal cells along their entire somatodendritic axis. Nat. Neurosci. *12*, 21–23.

Hevner, R.F., Shi, L., Justice, N., Hsueh, Y., Sheng, M., Smiga, S., Bulfone, A., Goffinet, A.M., Campagnoni, A.T., and Rubenstein, J.L. (2001). Tbr1 regulates differentiation of the preplate and layer 6. Neuron *2*, 353–366.

Hormuzdi, S.G., Pais, I., LeBeau, F.E., Towers, S.K., Rozov, A., Buhl, E.H., Whittington, M.A., and Monyer, H. (2001). Impaired electrical signaling disrupts gamma frequency oscillations in connexin 36-deficient mice. Neuron *31*, 487–495.

Itami, C., Kimura, F., and Nakamura, S. (2007). Brain-derived neurotrophic factor regulates the maturation of layer 4 fast-spiking cells after the second postnatal week in the developing barrel cortex. J. Neurosci. *27*, 2241–2252.

Iwasato, T., Nomura, R., Ando, R., Ikeda, T., Tanaka, M., and Itohara, S. (2004). Dorsal telencephalon-specific expression of Cre recombinase in PAC transgenic mice. Genesis *38*, 130–138.

Kanatani, S., Yozu, M., Tabata, H., and Nakajima, K. (2008). COUP-TFII is preferentially expressed in the caudal ganglionic eminence and is involved in the caudal migratory stream. J. Neurosci. *28*, 13582–13591.

Karagiannis, A., Gallopin, T., David, C., Battaglia, D., Geoffroy, H., Rossier, J., Hillman, E.M., Staiger, J.F., and Cauli, B. (2009). Classification of NPY-expressing neocortical interneurons. J. Neurosci. *29*, 3642–3659.

Kawaguchi, Y. (1995). Physiological subgroups of nonpyramidal cells with specific morphological characteristics in layer II/III of rat frontal cortex. J. Neurosci. *15*, 2638–2655.

Kill, I.R. (1996). Localisation of the Ki-67 antigen within the nucleolus. Evidence for a fibrillarin-deficient region of the dense fibrillar component. J. Cell Sci. *109*, 1253–1263.

Kriegstein, A.R., and Noctor, S.C. (2004). Patterns of neuronal migration in the embryonic cortex. Trends Neurosci. *27*, 392–399.

Kubota, Y., Hattori, R., and Yui, Y. (1994). Three distinct subpopulations of GABAergic neurons in rat frontal agranular cortex. Brain Res. *649*, 159–173.

Lai, T., Jabaudon, D., Molyneaux, B.J., Azim, E., Arlotta, P., Menezes, J.R., and Macklis, J.D. (2008). SOX5 controls the sequential generation of distinct corticofugal neuron subtypes. Neuron *57*, 232–247.

Lavdas, A.A., Grigoriou, M., Pachnis, V., and Parnavelas, J.G. (1999). The medial ganglionic eminence gives rise to a population of early neurons in the developing cerebral cortex. J. Neurosci. *19*, 7881–7888.

Lefebvre, V., Dumitriu, B., Penzo-Mendez, A., Han, Y., and Pallavi, B. (2007). Control of cell fate and differentiation by Sry-related high-mobility-group box (Sox) transcription factors. Int. J. Biochem. Cell Biol. *39*, 2195–2214.

Liodis, P., Denaxa, M., Grigoriou, M., Akufo-Addo, C., Yanagawa, Y., and Pachnis, V. (2007). Lhx6 activity is required for the normal migration and specification of cortical interneuron subtypes. J. Neurosci. *27*, 3078–3089.

Marin, O., and Rubenstein, J.L. (2001). A long, remarkable journey: tangential migration in the telencephalon. Nat. Rev. Neurosci. *2*, 780–790.

Marin, O., and Rubenstein, J.L. (2003). Cell migration in the forebrain. Annu. Rev. Neurosci. *26*, 441–483.

Marsh, E.D., Minarcik, J., Campbell, K., Brooks-Kayal, A.R., and Golden, J.A. (2008). FACS-array gene expression analysis during early development of mouse telencephalic interneurons. Dev. Neurobiol. *68*, 434–445.

Medvedev, A., Mackenzie, L., Hiscock, J.J., and Willoughby, J.O. (2000). Kainic acid induces distinct types of epileptiform discharge with differential involvement of hippocampus and neocortex. Brain Res. Bull. *52*, 89–98.

Miyoshi, G., Butt, S.J., Takebayashi, H., and Fishell, G. (2007a). Physiologically distinct temporal cohorts of cortical interneurons arise from telencephalic Olig2-expressing precursors. J. Neurosci. *27*, 7786–7798.

Miyoshi, G., Butt, S.J., Takebayashi, H., and Fishell, G. (2007b). Physiologically distinct temporal cohorts of cortical interneurons arise from telencephalic Olig2-expressing precursors. J. Neurosci. *27*, 7786–7798.

Montgomery, S.M., Sirota, A., and Buzsaki, G. (2008). Theta and gamma coordination of hippocampal networks during waking and rapid eye movement sleep. J. Neurosci. *28*, 6731–6741.

Nabbout, R., and Dulac, O. (2003). Epileptic encephalopathies: a brief overview. J. Clin. Neurophysiol. *20*, 393–397.

Nawa, H., Carnahan, J., and Gall, C. (1995). BDNF protein measured by a novel enzyme immunoassay in normal brain and after seizure: partial disagreement with mRNA levels. Eur. J. Neurosci. *7*, 1527–1535.

Nery, S., Fishell, G., and Corbin, J.G. (2002). The caudal ganglionic eminence is a source of distinct cortical and subcortical cell populations. Nat. Neurosci. *5*, 1279–1287.

Nobrega-Pereira, S., Kessaris, N., Du, T., Kimura, S., Anderson, S.A., and Marin, O. (2008). Postmitotic Nkx2-1 controls the migration of telencephalic interneurons by direct repression of guidance receptors. Neuron *59*, 733–745.

Okaty, B.W., Miller, M.N., Sugino, K., Hempel, C.M., and Nelson, S.B. (2009). Transcriptional and electrophysiological maturation of neocortical fast-spiking GABAergic interneurons. J. Neurosci. *29*, 7040–7052.

Pizzorusso, T., Medini, P., Berardi, N., Chierzi, S., Fawcett, J.W., and Maffei, L. (2002). Reactivation of ocular dominance plasticity in the adult visual cortex. Science *298*, 1248–1251.

Polleux, F., Whitford, K.L., Dijkhuizen, P.A., Vitalis, T., and Ghosh, A. (2002). Control of cortical interneuron migration by neurotrophins and PI3-kinase signaling. Development *129*, 3147–3160.

Popa, D., Popescu, A.T., and Pare, D. (2009). Contrasting activity profile of two distributed cortical networks as a function of attentional demands. J. Neurosci. *29*, 1191–1201.

Potter, G.B., Petryniak, M.A., Shevchenko, E., McKinsey, G.L., Ekker, M., and Rubenstein, J.L. (2009). Generation of Cre-transgenic mice using Dlx1/Dlx2 enhancers and their characterization in GABAergic interneurons. Mol. Cell. Neurosci. *40*, 167–186.

Powell, E.M., Mars, W.M., and Levitt, P. (2001). Hepatocyte growth factor/scatter factor is a motogen for interneurons migrating from the ventral to dorsal telencephalon. Neuron *30*, 79–89.

Rutherford, L.C., DeWan, A., Lauer, H.M., and Turrigiano, G.G. (1997). Brain-derived neurotrophic factor mediates the activity-dependent regulation of inhibition in neocortical cultures. J. Neurosci. *17*, 4527–4535.

Schwaller, B., Tetko, I.V., Tandon, P., Silveira, D.C., Vreugdenhil, M., Henzi, T., Potier, M.C., Celio, M.R., and Villa, A.E. (2004). Parvalbumin deficiency affects network properties resulting in increased susceptibility to epileptic seizures. Mol. Cell. Neurosci. *25*, 650–663.

Smits, P., Li, P., Mandel, J., Zhang, Z., Deng, J.M., Behringer, R.R., de Crombrugghe, B., and Lefebvre, V. (2001). The transcription factors L-Sox5 and Sox6 are essential for cartilage formation. Dev. Cell *1*, 277–290.

Sohal, V.S., Zhang, F., Yizhar, O., and Deisseroth, K. (2009). Parvalbumin neurons and gamma rhythms enhance cortical circuit performance. Nature *459*, 698–702.

Sousa, V.H., Miyoshi, G., Hjerling-Leffler, J., Karayannis, T., and Fishell, G. (2009). Characterization of Nkx6-2-derived neocortical interneuron lineages. Cereb. Cortex *19* (*Suppl 1*), i1–i10.

Srinivas, S., Watanabe, T., Lin, C.S., William, C.M., Tanabe, Y., Jessell, T.M., and Costantini, F. (2001). Cre reporter strains produced by targeted insertion of EYFP and ECFP into the ROSA26 locus. BMC Dev. Biol. *1*, 4.

Stenman, J., Toresson, H., and Campbell, K. (2003). Identification of two distinct progenitor populations in the lateral ganglionic eminence: implications for striatal and olfactory bulb neurogenesis. J. Neurosci. *23*, 167–174.

Stolt, C.C., Schlierf, A., Lommes, P., Hillgartner, S., Werner, T., Kosian, T., Sock, E., Kessaris, N., Richardson, W.D., Lefebvre, V., and Wegner, M. (2006). SoxD proteins influence multiple stages of oligodendrocyte development and modulate SoxE protein function. Dev. Cell *11*, 697–709.

Sugiyama, S., Di Nardo, A.A., Aizawa, S., Matsuo, I., Volovitch, M., Prochiantz, A., and Hensch, T.K. (2008). Experience-dependent transfer of Otx2 homeoprotein into the visual cortex activates postnatal plasticity. Cell *134*, 508–520.

Sussel, L., Marin, O., Kimura, S., and Rubenstein, J.L. (1999). Loss of Nkx2-1 homeobox gene function results in a ventral to dorsal molecular respecification within the basal telencephalon: evidence for a transformation of the pallidum into the striatum. Development *126*, 3359–3370.

Szabadics, J., Varga, C., Molnar, G., Olah, S., Barzo, P., and Tamas, G. (2006). Excitatory effect of GABAergic axo-axonic cells in cortical microcircuits. Science *311*, 233–235.

Tamamaki, N., Yanagawa, Y., Tomioka, R., Miyazaki, J., Obata, K., and Kaneko, T. (2003). Green fluorescent protein expression and colocalization with calretinin, parvalbumin, and somatostatin in the GAD67-GFP knock-in mouse. J Comp Neurol. *467*, 60–79.

Tamas, G., Lorincz, A., Simon, A., and Szabadics, J. (2003). Identified sources and targets of slow inhibition in the neocortex. Science *299*, 1902–1905.

Traub, R.D., Whittington, M.A., Stanford, I.M., and Jefferys, J.G. (1996). A mechanism for generation of long-range synchronous fast oscillations in the cortex. Nature *383*, 621–624.

Traub, R.D., Jefferys, J.G., and Whittington, M.A. (1997). Simulation of gamma rhythms in networks of interneurons and pyramidal cells. J. Comput. Neurosci. *4*, 141–150.

Tripodi, M., Filosa, A., Armentano, M., and Studer, M. (2004). The COUP-TF nuclear receptors regulate cell migration in the mammalian basal forebrain. Development *131*, 6119–6129.

Weiser, M., Bueno, E., Sekirnjak, C., Martone, M.E., Baker, H., Hillman, D., Chen, S., Thornhill, W., Ellisman, M., and Rudy, B. (1995). The potassium channel subunit KV3.1b is localized to somatic and axonal membranes of specific populations of CNS neurons. J. Neurosci. *15*, 4298–4314.

Wulff, P., Ponomarenko, A.A., Bartos, M., Korotkova, T.M., Fuchs, E.C., Bahner, F., Both, M., Tort, A.B., Kopell, N.J., Wisden, W., and Monyer, H. (2009). Hippocampal theta rhythm and its coupling with gamma oscillations require fast inhibition onto parvalbumin-positive interneurons. Proc. Natl. Acad. Sci. USA *106*, 3561–3566.

Xu, Q., Cobos, I., De La Cruz, E., Rubenstein, J.L., and Anderson, S.A. (2004). Origins of cortical interneuron subtypes. J. Neurosci. *24*, 2612–2622.

Xu, Q., Tam, M., and Anderson, S.A. (2008). Fate mapping Nkx2-1-lineage cells in the mouse telencephalon. J. Comp. Neurol. *506*, 16–29.

Zhao, Y., Marin, O., Hermesz, E., Powell, A., Flames, N., Palkovits, M., Rubenstein, J.L., and Westphal, H. (2003). The LIM-homeobox gene Lhx8 is required for the development of many cholinergic neurons in the mouse forebrain. Proc. Natl. Acad. Sci. USA *100*, 9005–9010.

Zhao, Y., Flandin, P., Long, J.E., Cuesta, M.D., Westphal, H., and Rubenstein, J.L. (2008). Distinct molecular pathways for development of telencephalic interneuron subtypes revealed through analysis of Lhx6 mutants. J. Comp. Neurol. *510*, 79–99.